Transient Response of Varying Thickness Timoshenko Beam under Point Load

by

Faisal Mahmood

A Thesis Presented to the

FACULTY OF THE COLLEGE OF GRADUATE STUDIES

KING FAHD UNIVERSITY OF PETROLEUM & MINERALS

DHAHRAN, SAUDI ARABIA

In Partial Fulfillment of the
Requirements for the Degree of

MASTER OF SCIENCE

In

MECHANICAL ENGINEERING

December, 1999

INFORMATION TO USERS

This manuscript has been reproduced from the microfilm master. UMI films the text directly from the original or copy submitted. Thus, some thesis and dissertation copies are in typewriter face, while others may be from any type of computer printer.

The quality of this reproduction is dependent upon the quality of the copy submitted. Broken or indistinct print, colored or poor quality illustrations and photographs, print bleedthrough, substandard margins, and improper alignment can adversely affect reproduction.

In the unlikely event that the author did not send UMI a complete manuscript and there are missing pages, these will be noted. Also, if unauthorized copyright material had to be removed, a note will indicate the deletion.

Oversize materials (e.g., maps, drawings, charts) are reproduced by sectioning the original, beginning at the upper left-hand corner and continuing from left to right in equal sections with small overlaps.

Photographs included in the original manuscript have been reproduced xerographically in this copy. Higher quality 6" x 9" black and white photographic prints are available for any photographs or illustrations appearing in this copy for an additional charge. Contact UMI directly to order.

Bell & Howell Information and Learning
300 North Zeeb Road, Ann Arbor, MI 48106-1346 USA
800-521-0600

TRANSIENT RESPONSE OF VARYING THICKNESS TIMOSHENKO BEAM UNDER POINT LOAD

BY

FAISAL MAHMOOD

A Thesis Presented to the

DEANSHIP OF GRADUATE STUDIES

KING FAHD UNIVERSITY OF PETROLEUM & MINERALS

DHAHRAN, SAUDI ARABIA

In Partial Fulfillment of the
Requirements for the Degree of

MASTER OF SCIENCE

In

MECHANICAL ENGINEERING

DECEMBER 1999

UMI Number: 1398761

UMI®

UMI Microform 1398761
Copyright 2000 by Bell & Howell Information and Learning Company.
All rights reserved. This microform edition is protected against
unauthorized copying under Title 17, United States Code.

Bell & Howell Information and Learning Company
300 North Zeeb Road
P.O. Box 1346
Ann Arbor, MI 48106-1346

KING FAHD UNIVERSITY OF PETROLEUM AND MINERALS

DHAHRAN 31261, SAUDI ARABIA

COLLEGE OF GRADUATE STUDIES

This thesis, written by **FAISAL MAHMOOD** under the direction of his Thesis Advisor and approved by his Thesis Committee, has been presented to and accepted by the Dean of the College of Graduate Studies, in partial fulfillment of the requirements for the degree of **MASTER OF SCIENCE IN MECHANICAL ENGINEERING**

THESIS COMMITTEE

Feb. 13, 2000
Dr. SAIF AL – KAABI (Chairman)

13-2-2000
Dr. MEHMET SUNAR (Member)

13-2-2000
Dr. YILBAS BEKIR (Member)

8-11-1420 H.
14-2-2000 G.
Dr. AHMED AL – GARNI (Member)

١٤٢٠/١١/٢٨
14/2/2000
Dr. YAGOUB AL – NASSAR (Member)

15/2/2000
Department Chairman

Dean, College of Graduate Studies

16-2-2000
Date

عمادة الدراسات العليا
DEANSHIP OF GRADUATE STUDIES

Acknowledgements

"In the name of Allah (God), Most Gracious, Most Merciful. Read, in the name of thy Lord and Cherisher, Who created man from a [leech-like] clot. Read, and thy Lord is Most Bountiful, He Who taught [the use of] the pen. Taught man that Which he knew not. Nay, but man doth Transgress all bounds. In that he looketh Upon himself as self-sufficient. Verily, to thy Lord Is the return [of all]." (The Holy QURAN, Surah no. 96)

Above and first of all, I thank and pray to Allah for His guidance and protection throughout my life, including the years of this study. I am happy to have had a chance to glorify His name, in the sincerest way, through this small accomplishment, and I ask Him, with hope only in Him, to accept my efforts. And secondly may peace be upon His Prophet, MOHAMMED(sala Allah Alaihe Wassalam).

I wish to dedicate this dissertation with heartful thanks to my parents, sisters, my wife, family members, friends, teachers and any person who supported or helped me in one way or another in this life.

I would like to express my sincere thanks to my advisor Dr. Saif Ahmed Al-Kaabi,

for sharing with me his profound knowledge and expertise in the field of wave propagation. This has been a great help during my studies at KFUPM. I also wish to thank him for his support, patience, comments, suggestions, constructive criticism and, ofcourse, encouragement.

I would also like to pay thanks the other members of my advisory committee: Dr. A. Al-Garni, Dr. M. Sunar, Dr. Y. Bekir and Dr. Y. Al-Nassar, who have been sincere and co-operative whenever i called. Hope this work will be just the onset of my research endeavor.

Dedicated

to

my PARENTS, SISTERS and WIFE

for

their moral support

Contents

List of Figures

Nomenclature

English Symbols

A	area of cross-section
$\hat{d}$	frequency dependant displacement vector
E	Young's modulus of material
$\hat{F}$	frequency dependant force vector
f_{min}	minimum prominent frequency in signal
G	shear modulus of material
h_{min}	minimum thickness of the beam
I	moment of inertia of cross-section
$\hat{k}_{ij}$	frequency dependant stiffness matrix element
k	wave number
L	beam length
l	elemental length

M	bending moment
$\hat{M}$	frequency dependant bending moment
Q	shear force
$\hat{Q}$	frequency dependant shear force
q	applied transient load
R	radius of curvature of neutral axis
y	lateral deflection
$\hat{y}$	frequency dependant lateral deflection

Greek Symbols

γ_0	shear strain at centroid
κ	shear correction factor
ω	circular frequency
ρ	density of material
ϕ	bending slope
η	damping coefficient

Abbreviations

FFT	Fast Fourier Transformation
IFFT	Inverse Fast Fourier Transformation
TR	Taper Ratio of beam thickness
PSD	Power Spectrum Density of signal

THESIS ABSTRACT

Name: FAISAL MAHMOOD

Title: TRANSIENT RESPONSE OF VARYING THICKNESS TIMOSHENKO BEAM UNDER POINT LOAD

Degree: MASTER OF SCIENCE

Major Field: MECHANICAL ENGINEERING

Date of Degree: DECEMBER 1999

Transient response of varying thickness beam is studied here numerically. Beam theory applied here includes effects of shear deformation and rotary inertia. The temporal and spatially dependant equations of motion are transferred to frequency domain by employing Fast Fourier Transformation (FFT). This resluts in the conversion of transient problem into pseudo-static problem. The ordinary differential equations (ODEs) thus obtained are then solved by the well established Finite Element methodology against each frequency within the band-limited signal. The frequency dependant response of beam at certain point, is then transferred back into the time domain by Inverse Fast Fourier Transformation (IFFT). Different types of boundary conditions applied here includes fixed-free, hinged-hinged an fixed-hinged. A special boundary condition, peculiar to wave propagation problem i.e: Throw-off element, is also applied. The response of uniform Timoshenko beam is validated with that for Euler beam obtained by analytical solution. The model developed here is demonstrated for two types of thickness variations i.e: linear and parabolic. The two modes of propagation are also studied under various damping values.

King Fahd University of Petroleum and Minerals, Dhahran.
DECEMBER 1999

ملخص الرسالة

الاسم : فيصل محمود

العنوان : الاستجابة العابرة لعتبة تيموشينكو متغيرة السمك بفعل الحمل النقطي

الدرجة : ماجستير في العلوم

التخصص : الهندسة الميكانيكية

التاريخ : ديسمبر ١٩٩٩ مـــ

لقد تم في هذا البحث دراسة الاستجابة العابرة للعتبات المعدنية متغيرة السمك بتضمين تأثير التشـــوه القصـــي و القصور الذاتي الدوراني. في البداية تم تحويل معادلات الحركة من المجال الزمني إلى المجال الترددي باستخدام طريقة فورييه للتحويل السريع، ومن ثم حلت المعادلات التفاضلية الناتجة باستخدام طريقة العنصر المحدد وذلـــك لكـــل ذبذبة ترددية. ناتج حل المسألة الجبرية هو الاستجابة الترددية للعتبة عند نقطة معينة و التي حولت مرة أخـرى إلى المجال الزمني باستخدام طريقة فورييه العكسية للتحويل السريع. اشتملت هذه الدراسة على الاهتمام بعدة أنـــواع من الأوضاع الحدية وهي الحدود المثبتة و المدعم البسيط و الحر و مجموعة مؤتلفة من هـــذه الأنـــواع. كمـــا اشتملت الدراسة على استخدام نوع خاص من الأوضاع الحدية وهو ما يسمى بعنصر الفصل. كما تم الاهتمـــام في هذا البحث بدراسة نوعين من السمك المتغير : الخطي و المنحنى المكافئ، كذلك اشتمل البحث على دراســـة تأثير التخميد على انتشار الموجات في العتبات.

جامعة الملك فهد للبترول و المعادن

الظهران،المملكة العربية السعودية

ديسمبر ١٩٩٩

Chapter 1

INTRODUCTION

Wave phenomenon is a source of information on the properties of solids, be these solids the earth, pure crystals of metals, or other substances. The behavior of structural materials under load causing permanent deformation is found in various aspects of military and space technology. Metal forming processes such as explosive forming, forging and sonic riveting also fall in the same category. Crack propagation or the interaction of dynamic stress fields with existing crack or voids is an area of study in the structures. The field of ultrasonic represents another major area of application of wave phenomenon. The general aspects of this area involve introducing a very low energy level, high frequency stress pulse into material and observing the subsequent propagation and reflection of this energy. Propagation, reflection and attenuation of ultrasonics determines fundamental properties of materials such as elastic constants and damping characteristics. Non-destructive testing (NDT)

makes wide use of ultrasonics for the determination and characterization of defects in critical structures. These techniques are used widely in aerospace, transportation, chemical and energy industries. Such tests are needed in both the manufacturing phases of products in order to assume quality as well as during the operating life-time of the products in order to predict and hence prevent failure. Waves in earth is an interesting area of propagation phenomenon. Study of the waves generated by earthquakes or artificially produced tremors provide the most knowledge on the interior construction of earth. By studying the reflection of waves from underground discontinuities, it is possible to locate possible oil bearing deposits.

Rods and beams are the most important structural elements and form the basis of many truss and grid frame works. In structural design, beams of non-uniform cross-section are often encountered. Usually beams are designed with non-uniform cross-section with view of reducing cost and weight. In civil engineering structural design towers, arches, chimneys and bridge girders are examples of tapered beams. In aerospace structural design, nearly all beams/plates are tapered e.g. wings are tapered for both weight and aerodynamic reasons. In automotive structural design, examples can be found in the suspension systems where beams are designed in leaf-spring type. Such a design can save material and produce the desirable structural damping. The response of a system is governed by three system parameters: damping, mass and stiffness. The influence of damping is most prominent at resonance and higher frequencies.

In the present work, transient wave propagation analysis in varying thickness Timoshenko beams will be studied under general point load. Firstly, equations of motion will be derived. Then transient response will be evaluated using finite element method, both conventional and spectral. Various boundary conditions and thickness variations are considered.

1.1 LITERATURE REVIEW

Most of the work in the field of structural beam response, is mainly focused on the vibration analysis. The main difference between vibration and wave propagation analysis lies in the frequency components of the signal. On wave propagation analysis frequencies dealt are well above the frequencies used in vibration analysis. Also in vibration analysis we are, in general, concerned only with natural frequencies and mode shapes but not with the response of the system, and there is only one independent variable i.e: the temporal parameter in vibration case. However in wave propagation both temporal and spectral parameters are taken into account. Dynamic analysis applied to beams, can be can be classified into two categories:

1. Analysis of Euler-Bernoulli beams

2. Analysis of Timoshenko beams

1.1.1 EULER BEAM

If the lateral dimensions of the beam are less than $\frac{1}{10}$th of its length, then the effects of shear deformation and rotary inertia can be ignored. Beam based on such condition is called Euler-Bernoulli beam or thin beam. Goel [1] investigated the transverse vibrations of the linearly tapered beams, elastically restrained against rotation at either end. He presented numerical results of the first three eigen frequencies with different stiffness and taper ratios. Roy [2] conducted a detailed study on the effect of different thickness profile variations on the amplitude of deflection and the dynamic bending stress of cantilever beam under a point harmonic load. After comparing with uniform thickness beam, he observed that considerable reduction in amplitude and/or bending stress can be achieved by proper selection of thickness variation. Ting [3] developed a stiffness matrix for a beam on elastic foundation, and element load vectors due to concentrated forces for plane frame analysis. They also presented an element flexibility matrix and element displacement vectors, for the force method, due to aforementioned loads. They derived stiffness and flexibility matrices from the exact solution of the differential equation and their finite element analysis results are exact for the Navier and Winkler assumptions. Carnegie [4] presented a method with strong convergence characteristics for the determination of eigenvalues and eigenvectors of the continuous systems. To remove the limitation on the number of undetermined constants in the displacement functions introduced

by the conditions at the ends of a segment, he introduced points of freedom within the segment. He concluded that this method is particularly useful in analyzing the vibration of beams carrying concentrated masses and beams on elastic supports. According to his suggestion this analysis can be extended to vibration problems of non-uniform, pre-twisted asymmetric beams and to plates and shells. Chin et al [5] developed stiffness and mass matrices of the beam on elastic foundation element from the exact solution of the shape functions governing its end deformations. The mass and stiffness matrices are then combined with those of conventional beam element to obtain assembled mass and stiffness matrices, which can be used to determine natural frequencies and mode shapes of a general structure.

1.1.2 TIMOSHENKO BEAM

Timoshenko [6] was the first one who proposed to show the effect of shear in investigating transverse vibrations. He deduced the general equation of vibration of the prismatic bars from which Euler-Bernoulli differential equation can be obtained as special cases. Based on Timoshenko differential equation for the transverse bending of elastic beams, Dangler [7] obtained closed form solutions for the stresses induced in a long uniform beam, by the action of an impulsive, concentrated transverse load. Kapur [8] extended finite element method, for the solution of problems in structural mechanics, to vibrations of beams including shear and rotary inertia effects. Using consistent mass matrix in conjunction with the corresponding stiffness matrix, he

concluded that his method satisfactorily encompasses all boundary conditions for a Timoshenko beam and his results showed excellent agreement with the exact solution. He claimed that his method is directly applicable to non-uniform beams under various boundary conditions. Eagle [9] developed a beam theory which included the effects of transverse shear deformation and rotary inertia and whose kinetic and potential energies may be written in terms of a single dependant variable. Neglecting the coupling between the transverse shear deformation and rotary inertia, the natural frequencies obtained by his method show excellent agreement with those of the Timoshenko theory. Franklin et al [10] derived differential equations, stiffness coefficients and fixed end forces, for general analysis of structural systems, the constituent members of which may have transverse and rotary inertia, shear and bending deformation, axial force and elastic foundation. They illustrated numerical procedures for determining natural frequencies and dynamic response and presented their results for various typical beams. To [11] developed explicit mass and stiffness matrices of a linearly tapered beam finite element, in order to provide a means of incorporating, as well as, investigating, the effect of secondary contributions of shear deformation and rotary inertia in vibration analysis of class of mast antenna structures, and to determine the aspect ratio criterion of tapered cantilever beam structures. Nakao [12] discussed the forced vibration of an anisotropic, viscoelastic Timoshenko beam with free ends, both theocratically and experimentally. He introduced damping factors associated with dynamic Young's modulus and shear

modulus, separately in the equation. Heppler and Hansen [13] developed Timoshenko beam finite element model using trignometric basis function. The properties and performance of this new model are explored through a series of illustrative problems that treat both straight and curved geometries. The results obtained from this work indicate that the trignometric basis functions are a competitive alternative to polynomial basis functions with regard to accuracy and convergence. Thomas and Abbas [14] presented for the first time a finite element model with nodal degrees of freedom which can satisfy the forced and natural boundary conditions of a Timoshenko beam. The mass and stiffness matrices of the element are derived from kinetic and strain energies by assigning polynomial expressions for the total deflection and bending slope. They showed very rapid convergence of the results obtained from their model and concluded that relatively less number of elements is required to obtain good results. To analyze small amplitude, free vibration of non-uniform beams on variable two parameter foundations, Hou and Tseng [15] developed a new finite element model for Timoshenko beam. An important characteristic of the model is that the cross-sectional area, the second moment of area, the winkler foundation modulus and shear foundation modulus are all assumed to vary in polynomial forms, implying that beam element can deal with circular, tubular and even complex sections as well as the foundation of beams which vary in a general way. Lindberg [16] derived a stiffness matrix for any non-uniform beam. He found excellent results in the case of linearly varying cantilever beam with very few

elements.

Some research studies have been carried out numerically for wave propagation through structural beams and rods. Broadly speaking, the studies can be classified into two categories:

1. Conventional finite element analysis

2. Spectral finite element analysis

Calif [17] presented a new method for deriving flexural wave solutions for the uniform Timoshenko bending theory. His method is based on a breakdown of the total deflection into its bending and shear components. Instead of treating the full Timoshenko equation an equivalent set of coupled equations, representing the rotational and translatory motions of the beam element, is solved. Lee [18] introduced a new continuum modeling method, by the use of spectral element, for the large truss type periodic space structures that are expected to operate at relatively low frequency. Before adopting the spectral element in the continuum modeling procedure, the inherent accuracy of the spectral element is discussed in comparison with the conventional finite element, which has been used previously in continuum modeling method. He showed that results are in good agreement with those obtained from other continuum method. Doyle [19] showed how a spectral formulation for a dynamic finite element can model the distributed mass exactly, allowing elements to span from joint to joint, thus saving computing power and time. He demonstrated

the versatility of this approach in terms of modeling viscoelastic rods, tapered rods, trusses etc.

In the above studies, beams were treated for wave propagation where harmonic excitation were assumed at very low frequency. It seems that no work has been performed to investigate the wave propagation in Timoshenko beams of varying thickness due to a transient point force.

1.2 OBJECTIVE OF PRESENT WORK

A new approach is adopted for the non-uniform Timoshenko beams analysis by using spectral finite elements. In this approach, first the beam is divided into a number of elements so that each element may be treated as uniform, and then displacement vector is transformed from time domain into frequency domain using Fast Fourier Transformation (FFT). This transformed response is fed back into the governing differential equations of the beam. The equations resulted contain space as the only independent variable. The resulting ordinary differential equations (ODEs) are solved at each frequency component, using Finite Element method, and the transient response (in time domain) is recovered by using the inverse FFT. The effects of different types of boundary conditions (e.g. fixed-free, hinged-hinged) and thickness variations (linear and parabolic) are also studied.

Chapter 2

THEORETICAL FORMULATION

If the cross-sectional dimensions are not small compared to the length of the beam, we need to consider the effect of rotary inertia and shear deformation. In 1921 Timoshenko [6] included the effects of both shear and rotary inertia and obtained results in accord with exact theory. The procedure, presented by Timoshenko is known as the thick beam theory or Timoshenko beam theory. The study of wave propagation in the elementary (thin) beam theory, the Bernoulli-Euler beam theory, showed that unrealistic infinite phase velocities were predicted at high frequencies. Looking at the assumptions in deriving this theory, neglecting the rotary inertia effects is an obvious failing. At very high frequencies the contribution of the rotational acceleration could be significant. A subtler assumption used in the elementary theory is

that the shear deformation is zero; even though there is shear force. Both of these assumptions will be relaxed in the present high-order Timoshenko beam theory.

2.1 GENERAL ASSUMPTIONS

The present study is mainly based on the following basic assumptions:

1. Beam is initially straight and unstressed.
2. The material of the beam is perfectly elastic, homogeneous and isotropic.
3. Every cross-section of the beam is symmetrical about the plane of bending i.e.: about an axis perpendicular to the neutral axis.
4. There is no resultant force perpendicular to any cross-section.
5. Plane sections remain plain during bending, but no longer perpendicular to the centroidal plane. Accordingly, warping of the cross-section is no longer present. Thus, shear deformation will be considered.
6. Relationship between bending moment and curvature as assumed in elementary theory still exists.
7. The effects of rotary inertia are included.
8. The deflections are small compared to the beam thickness.
9. Material properties are kept constant in the analysis.

2.2 GOVERNING EQUATIONS

Consider an element of beam subjected to shear force, bending moment and distributed load as shown in Figure (2.1)

The transverse displacement is measured by $y \equiv y(x,t)$ and the slope of the centroidal axis is given by $\frac{\partial y}{\partial x}$. This slope is considered to be made of two contributions. The first is $\phi \equiv \phi(x,t)$, due to the effects of bending. An additional contribution is γ_0, which defines the shear strain due to shearing effects.

Thus we have:

$$\frac{\partial y}{\partial x} = \phi + \gamma_0 \tag{2.1}$$

Now we relate the above kinematic expression to the loads using assumption 2, in terms of present parameters:

$$\frac{M}{EI} = \frac{-1}{R} \tag{2.2}$$

where R is the radius of curvature, M is the bending moment at the cross-section under consideration and E is the modulus of elasticity of the material.

For small curvature:

$$Rd\phi = dx \tag{2.3}$$

or

$$\frac{1}{R} = \frac{d\phi}{dx} \tag{2.4}$$

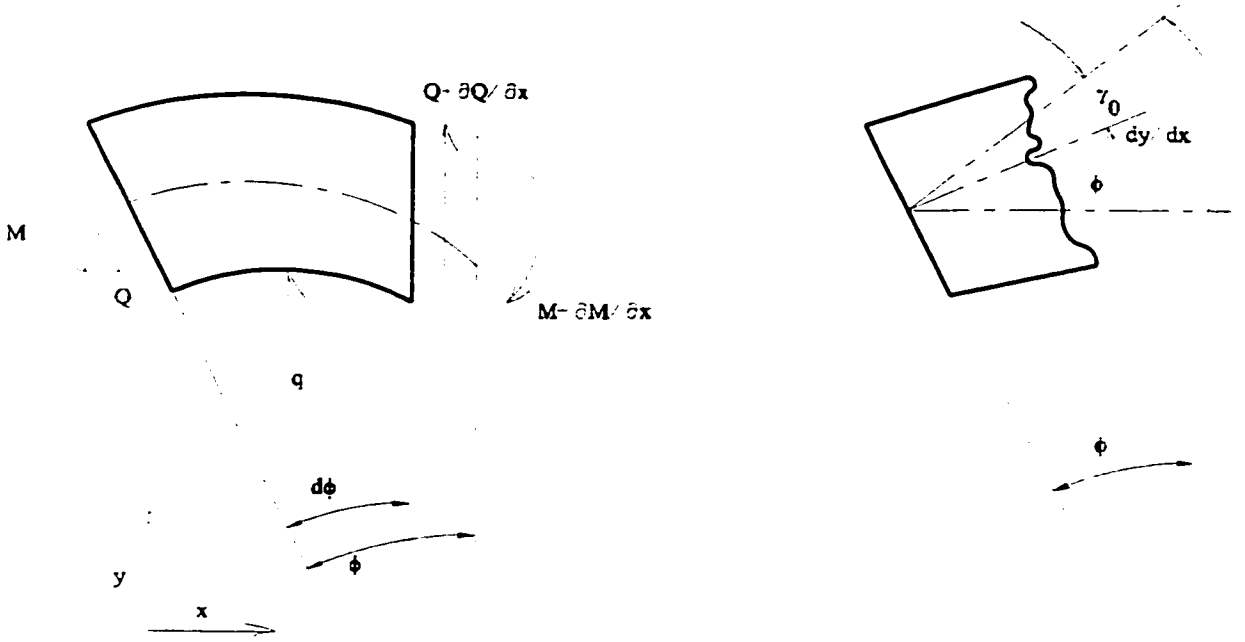

Figure 2.1: Differential element of the beam subjected to load and kinematical details of additional shearing deformation

From equation (2.2) we get:

$$\frac{M}{EI} = \frac{-\partial \phi}{\partial x} \tag{2.5}$$

The shear force, Q, at the cross-section is given in terms of the shear stress, τ or shear strain , γ, as:

$$Q = \int_A \tau dA = G \int_A \gamma dA \tag{2.6}$$

where G defines the material modulus of rigidity, which is assumed to be constant and $A \equiv A(x)$ is the area of cross-section.

As γ_0 is defined as the shear strain at the centroidal axis, then $G\gamma_0 A$ will give a shear force. To account for the fact that shear is not constant across the thickness, a correction factor, κ (Timoshenko shear factor) is introduced such that:

$$Q = G \int_A \gamma dA = G\gamma_0 \kappa A \tag{2.7}$$

The value of κ will depend on the shape of the cross-section and must be determined, usually by stress analysis means, for each cross-section. In the present study, κ is taken to be equal to $\frac{2}{3}$. By substituting equation (2.1) into equation (2.7) we obtain

$$Q = AG\kappa(\frac{\partial y}{\partial x} - o) \tag{2.8}$$

Now writing the equation of motion in vertical direction, we obtain

$$-Q + (Q + \frac{\partial Q}{\partial x}dx) + qdx = \rho A dx \frac{\partial^2 y}{\partial t^2} \tag{2.9}$$

Where $q \equiv q(x,t)$, is the distributed force. Simplifying equation (2.9), we get:

$$\frac{\partial Q}{\partial x} + q = \rho A \frac{\partial^2 y}{\partial t^2} \tag{2.10}$$

summing moments about an axis perpendicular to x-y plane and passing through the center of element, we get:

$$M - (M + \frac{\partial M}{\partial x}dx) + \frac{1}{2}Qdx + \frac{1}{2}(Q + \frac{\partial Q}{\partial x}dx)dx = J\frac{\partial^2 \phi}{\partial t^2} \tag{2.11}$$

where $J \equiv J(x)$ is the polar moment of inertia and is equal to $\rho I dx$, where $I \equiv I(x)$, is second moment of area.

From equation(2.11)

$$Q - \frac{\partial M}{\partial x} = \rho I \frac{\partial^2 \phi}{\partial t^2} \tag{2.12}$$

Substituting equations (2.5) and(2.8) into the equations (2.10) and (2.12) gives:

$$G\kappa(\frac{\partial A}{\partial x}(\phi - \frac{\partial y}{\partial x}) + A(\frac{\partial \phi}{\partial x} - \frac{\partial^2 y}{\partial x^2})) + \rho A \frac{\partial^2 y}{\partial t^2} = q(x,t) \tag{2.13}$$

and

$$GA\kappa(\frac{\partial y}{\partial x} - \phi) + E(\frac{\partial I}{\partial x}\frac{\partial \phi}{\partial x} + I\frac{\partial^2 \phi}{\partial x^2}) = \rho I \frac{\partial^2 \phi}{\partial t^2} \tag{2.14}$$

Equations (2.13) and (2.14) are the governing equations of motion of Timoshenko beam of varying thickness.

2.3 DISPERSION RELATIONS FOR UNIFORM THICKNESS BEAM

Dispersion relation shows the relation between the phase velocity and the frequency of the harmonic wave. It determines the change of shape of the travelling wave. For constant thickness Timoshenko beam, the equations of motion (equations (2.13) and (2.14)) can be written as, letting $q = 0$:

$$GA\kappa\left[\frac{\partial^2 y}{\partial x^2} - \frac{\partial o}{\partial x}\right] = \rho A\frac{\partial^2 y}{\partial t^2} \tag{2.15}$$

$$EI\frac{\partial^2 o}{\partial x^2} + GA\kappa\left[\frac{\partial y}{\partial x} - o\right] = \rho I\frac{\partial^2 o}{\partial t^2} \tag{2.16}$$

There are two dependant variables y, o and the coefficients are constants.

Assuming harmonic waves, the solution can be written as:

$$y = y_0 e^{-i(kx-\omega t)} \tag{2.17}$$

$$o = o_0 e^{-i(kx-\omega t)} \tag{2.18}$$

Where y_0 and o_0 are the amplitudes.

Substituting equations (2.17) and (2.18) into equations (2.15) and (2.16) we get:

$$\begin{bmatrix} GA\kappa k^2 - \rho A\omega^2 & -ikGA\kappa \\ ikGA\kappa & EIk^2 + GA\kappa - \rho I\omega^2 \end{bmatrix}\begin{bmatrix} y_0 \\ o_0 \end{bmatrix} = 0 \tag{2.19}$$

Defining

$$c_1 \equiv \sqrt{\frac{EI}{\rho A}}$$

$$c_2 \equiv \sqrt{\frac{GA\kappa}{\rho A}}$$

$$c_3 \equiv \sqrt{\frac{\rho I}{\rho A}}$$

So we have from equation (2.19)

$$\begin{bmatrix} \left(k^2 - \frac{\omega^2}{c_2^2}\right) & -ik \\ ik & \left(\frac{k^2 c_1^2}{c_2^2} + 1 - \frac{\omega^2 c_1^2}{c_2^2}\right) \end{bmatrix} \begin{bmatrix} y_0 \\ \phi_0 \end{bmatrix} = 0 \tag{2.20}$$

For nontrivial solution determinant must be zero, so we obtain from equation (2.20)

$$k^4 - k^2\omega^2 \left[\left(\frac{1}{c_2}\right)^2 + \left(\frac{c_3}{c_1}\right)^2\right] - \left[\left(\frac{\omega}{c_1}\right)^2 - \left(\frac{c_3}{c_2 c_1}\right)^2 \omega^4\right] = 0 \tag{2.21}$$

Solving for k, we get

$$\begin{aligned} k^2 &= \frac{1}{2}\left[\left(\frac{1}{c_2}\right)^2 + \left(\frac{c_3}{c_1}\right)^2\right]\omega^2 \\ &\quad \pm\sqrt{\left(\frac{\omega}{c_1}\right)^2 + \frac{1}{4}\left[\left(\frac{1}{c_2}\right)^2 - \left(\frac{c_3}{c_1}\right)^2\right]^2 \omega^4} \end{aligned} \tag{2.22}$$

Therefore, there are four modes of wave propagation. Equation (2.22) is the dispersion equation for constant thickness Timoshenko beam. Dispersion curves representing the solution of equation (2.22) are shown in Figure (2.2)

At very small frequency, in comparison with the cut off frequency of second mode:

$$k_1 \approx \pm\sqrt{\frac{\omega}{c_1}}$$

$$k_2 \approx \pm i\sqrt{\frac{\omega}{c_1}}$$

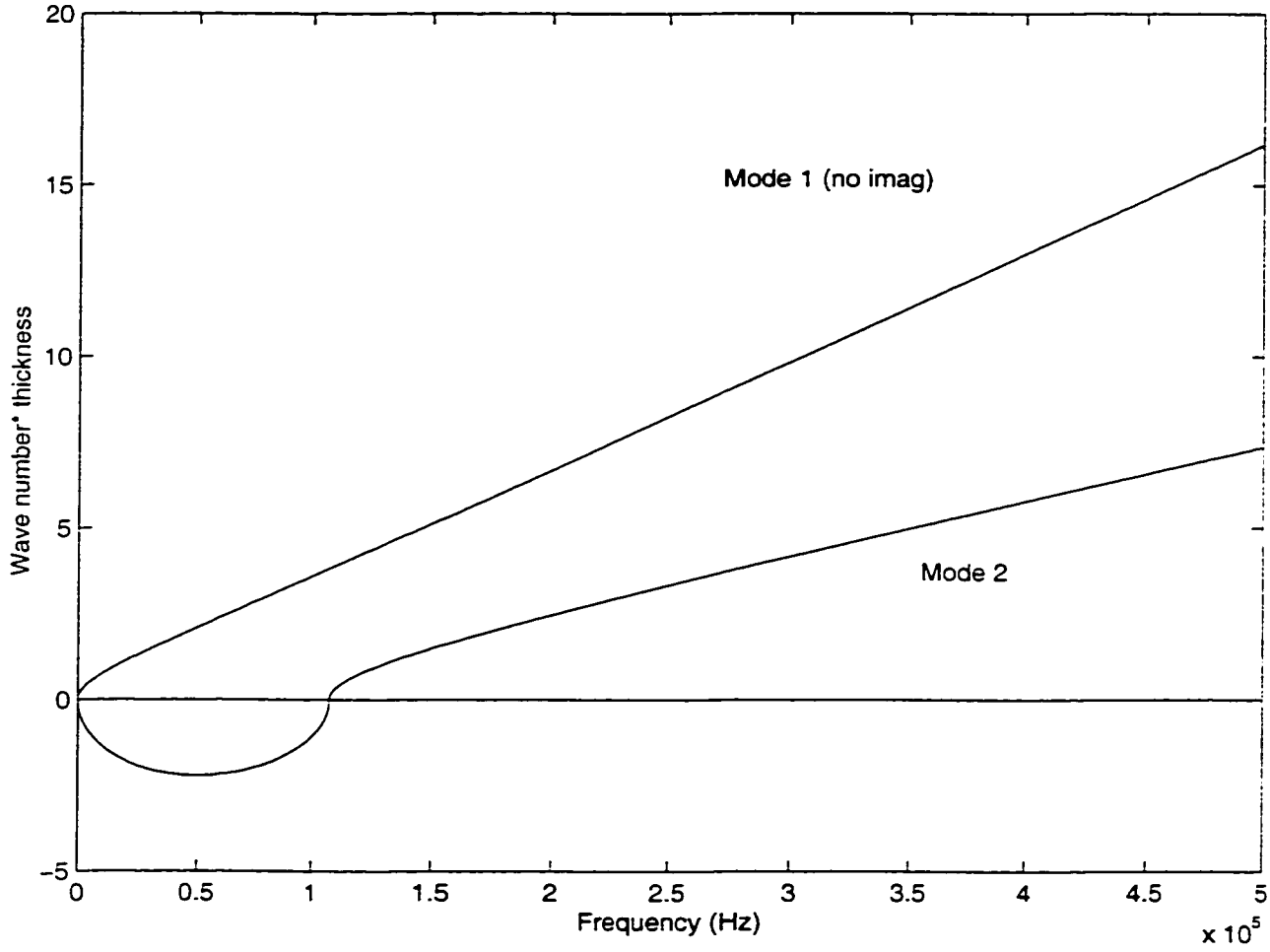

Figure 2.2: Dispersion relation for uniform Timoshenko beam

so modes are independent of $GA\kappa$ and ρI and that is why this high-order theory does not introduce additional modes. On the other hand, as the frequency becomes very large then:

At high frequency:

$$k_1 \Longrightarrow \frac{\omega}{c_2}$$

$$k_2 \Longrightarrow \frac{c_3}{c_1}\omega$$

k_1 and k_2 are the propagating modes, hence imaginary branch must have turned real. Cutoff frequency of the second mode, ω_0, is obtained where k is zero and this is found to be where:

$$\omega_0 = \frac{c_2}{c_3} = \sqrt{\frac{GA\kappa}{\rho I}}$$

To eliminate the rotational inertia, it is necessary to let $c_3 = 0$ and to eliminate the shear deformation to let $c_2 = \infty$. In both cases the cut-off frequency goes to infinity giving the second mode only evanescent.

Chapter 3

SPECTRAL FINITE ELEMENT FORMULATIONS

The use of conventional finite element analysis for the dynamic problems, requires substantially large number of elements than needed for the equivalent static problem. This enables mass distribution adequately at the nodes. To model the mass distribution exactly for the dynamic problem, the finite element model using spectral formulation was developed by Doyle [20] and is used in this work. The major significance of the method is that it allows elements to span from joint to joint, thus the subdivision of the member into many small elements is no longer needed.

3.1 TEMPORAL DISCRETE FOURIER TRANSFORM

Although the temporal Fourier transform methods are well developed and well documented, we will review the basic concepts for completeness. Let us us assume that $y(t)$ describes the response at any position and it is a function of time t only. Then, the temporal Fourier transform of $y(t)$ is given by

$$Y(f) = \int_{-\infty}^{\infty} y(t) e^{-i2\pi ft} dt \tag{3.1}$$

Where f is the frequency ($\omega = 2\pi f$). In the most common situations, $y(t)$ is sampled at evenly spaced intervals in time. Let Δt denote the sampling interval (time interval between consecutive samples) and suppose that we have N consecutive sampled values, then

$$y_j = y(j\Delta t)$$

quation where $j = 0, 1, 2, \ldots, N-1$

The Fourier transform $Y(f)$ is estimated at the following discrete frequencies

$$f_n = \frac{n}{N\Delta t} \tag{3.3}$$

Where $n = -\frac{N}{2}, \ldots, \frac{N}{2}$ The integral in equation (3.1) is approximated by a discrete sum as:

$$Y(f_n) \approx \sum_{j=0}^{N-1} y_j e^{-2i\pi f_n t_j} \Delta t = \Delta t \sum_{j=0}^{N-1} y_j e^{-2i\pi j \frac{n}{N}} \tag{3.4}$$

Now we need to know how the sampling rate ($\frac{1}{\Delta t}$) can be determined. For any sampling interval Δt, there is also a special frequency f_c, called the Nyquist frequency, which is related to Δt by:

$$\Delta t = \frac{1}{2f_c} \tag{3.5}$$

Practically, f_c is the maximum frequency contained in the signal. If a continuous function $y(t)$, sampled at an interval Δt, happens to be band-width limited to frequencies smaller in magnitude than f_c i.e. if $H(f) = 0$ for all $|f| > f_c$, then the function $y(t)$ is completely determined by its samples y_j. However, if a function is not sampled at a rate $\frac{1}{\Delta t}$ equal to or higher than $2f_c$, a problem called aliasing results. Any frequency component outside of the frequency range $(-f_c, f_c)$ is aliased (falsely translated) into that range by the very act of discrete sampling. Another expected problem from using the discrete Fourier transform is leakage which causes the appearance of sidelobes around the maximum peak of the power spectrum. Leakage occurs if the amplitudes and slopes of the sampled signal are not the same at the start and end of the sampled data. This happens when the frequency of the sampled signal is not equal to one of the discrete frequencies f_n's in equation (3.3). The solution to the problem of leakage is the use of so-called data windowing.

3.2 SPECTRAL REPRESENTATION OF TERMS

The spectral approach finds its most fruitful application in the analysis of experimental data from the real system. The key to the spectral description of waves is to be able to express the phase changes incurred as the wave propagates from location to location. This is done conveniently through the use of differential equations for particular models. The idea of representing the time variation of a function by a summation of harmonic functions is extended here to representing arbitrary functions of time and position resulting from the solution of wave equations. The approach is to remove the time variation by using the spectral representation of the solution. This leaves a new differential equation for the coefficients, which in many cases can be integrated directly.

3.2.1 GENERAL FUNCTIONS

The solutions in the wave problems are general functions of space and time. If the time variation of the solution is focused on at a particular point in space, then it has the spectral representation

$$u(x_1, y_1, t) = f_1(t) = \sum C_{1n} e^{i\omega_n t} \tag{3.6}$$

At another point, it behaves as a time function $f_2(t)$ and is represented by the Fourier coefficients C_{2n}. That is, the coefficients are different at each spatial point.

Thus, the solution at any arbitrary position has the following spectral representation

$$u(x,y,t) = \sum_n \hat{u}_n(x,y,\omega_n)\, e^{i\omega_n t} \tag{3.7}$$

Where $\hat{u}_n$ are the spatially dependant Fourier coefficients. These coefficient are functions of frequency ω and thus there is no reduction in the total number of independent variables.

For shorthand, the summation and subscripts are omitted and the function will be given the representation

$$u(x,y,t) \Longrightarrow \hat{u}(x,y,\omega) \tag{3.8}$$

Sometimes it is written simply as $\hat{u}$.

3.2.2 DERIVATIVES

The differential equations are given in terms of both space and time derivatives. Since they are linear, then it is possible to apply the spectral representation to each term appearing. Thus, the spectral representation for the time derivative is

$$\frac{\partial u}{\partial t} = \frac{\sum \hat{u}_n e^{i\omega_n t}}{\partial t} = \sum i\omega_n \hat{u}_n e^{i\omega_n t} \tag{3.9}$$

In shorthand, this becomes

$$\frac{\partial u}{\partial t} \Longrightarrow i\omega\hat{u} \tag{3.10}$$

In fact, time derivatives of general order have the representation

$$\frac{\partial^m u}{\partial t^m} \Longrightarrow i^m \omega^m \hat{u} \tag{3.11}$$

So the algebraic expressions in the Fourier coefficients replace the time derivatives. That is, there is reduction in the number of derivatives occurring.

Similarly, the spatial derivatives are represented by

$$\frac{\partial u}{\partial x} \Longrightarrow \frac{\partial \hat{u}}{\partial x} \tag{3.12}$$

In this case there appears no reduction, but with the removal of time as an independent variable, these derivatives often become ordinary derivatives, and thus more amenable to integration.

3.3 POWER SPECTRAL DENSITY

The total power in a signal is the same whether we compute it in time domain or in frequency domain, so:

Total Power $= \int_{-\infty}^{\infty} |y(t)|^2 \, dt = \int_{-\infty}^{\infty} |Y(f)|^2 \, df$

To find the power contained in the frequency interval between f and $f + df$, with f varying from 0 to $+\infty$, the one sided power spectral density (PSD) of the function y is defined as:

$$P_y(f) \equiv |Y(f)|^2 + |Y(-f)|^2 \, , 0 \leq f \leq \infty \tag{3.13}$$

so that the total power is just the integral of $P_y(f)$ from $f = 0$ to $f = \infty$. When function $y(t)$ is real then the two terms in equation (3.13) are equal, so $P_y(f) = 2|Y(f)|^2$. If a function $y(t)$ goes endless from $-\infty$ to ∞ then its total power and PSD will in general be infinite. Of interest is then PSD per unit time.

This is computed by taking a long, but finite stretch of the function $y(t)$. computing its PSD (i.e; PSD of a function which is equal to $y(t)$ in the finite stretch but is zero everywhere else); and then dividing the resulting PSD by the length of stretch used. Figure (3.1) shows a signal and its PSD. From the PSD curve one can determine the low and high frequency limits of the signal.

3.4 DYNAMIC STIFFNESS

The spectral formulation begins with the equations of motion of the Timoshenko beam including inertia terms. Mass is no longer concentrated at the nodes. It is assumed that there are no applied loads between the element ends.

Dividing the beam into a number of elements, cross-sectional area and second moment of area at the mid of each element can then be considered to be constant over the entire element. So the equations of motion of Timoshenko beam can be written as:

$$GA\kappa\left[\frac{\partial^2 y}{\partial x^2} - \frac{\partial \phi}{\partial x}\right] = \rho A\frac{\partial^2 y}{\partial t^2} - q \tag{3.14}$$

$$EI\frac{\partial^2 \phi}{\partial x^2} + GA\kappa\left[\frac{\partial y}{\partial x} - \phi\right] = \rho I\frac{\partial^2 \phi}{\partial t^2} \tag{3.15}$$

The displacement and the bending slope are given by their spectral representation:

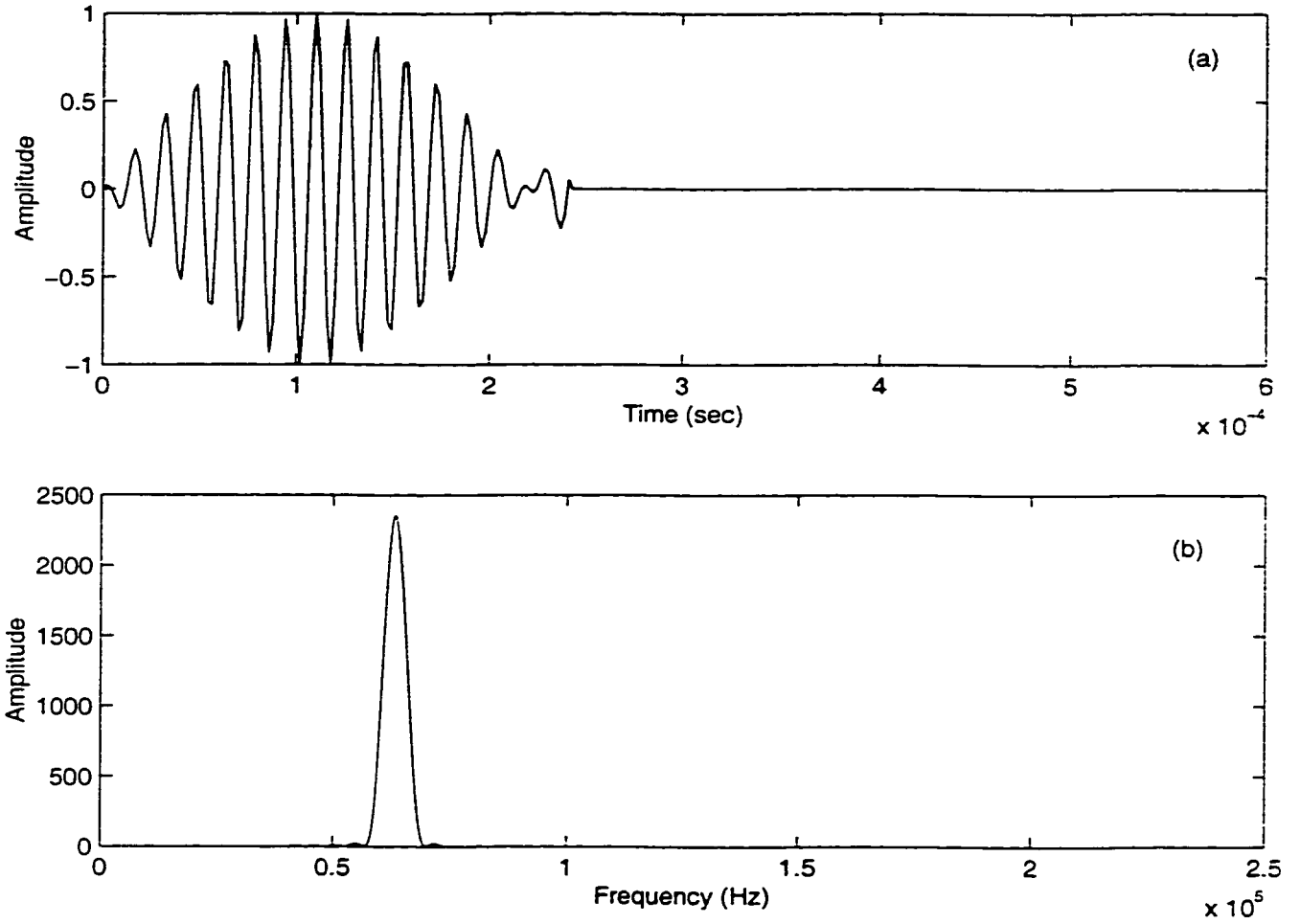

Figure 3.1: A signal and its Power Spectrum Density

$$\begin{aligned} y(x,t) &= \sum_n \hat{y}_n(x,\omega_n)\, e^{i\omega_n t} \\ \phi(x,t) &= \sum_n \hat{\phi}_n(x,\omega_n)\, e^{i\omega_n t} \end{aligned} \tag{3.16}$$

The spectral components $\hat{y}_n$ and $\hat{\phi}_n$ have the simple solution:

$$\hat{y}_n = A_1 e^{-ik_1 x} + B_1 e^{-ik_2 x} + C_1 e^{ik_1 x} + D_1 e^{ik_2 x} \tag{3.17}$$

$$\hat{\phi}_n = A_2 e^{-ik_1 x} + B_2 e^{-ik_2 x} + C_2 e^{ik_1 x} + D_2 e^{ik_2 x} \tag{3.18}$$

Where k_1 and k_2 are the wave numbers given in the previous chapter and A_1, A_2, B_1, B_2 etc. are the frequency dependant coefficients and are complex in nature.

The first two terms in the above equations describe waves moving in the forward direction while the last two describe backward moving waves. Both sets are necessary since the element is finite. Either $\hat{y}_n$ or $\hat{\phi}_n$ can be chosen, we used here $\hat{\phi}_n$ as the working variable.

Putting $\hat{y}_n$ and $\hat{\phi}_n$ in equation (3.14) considering the load to be applied at the nodes only we have

$$GA\kappa\left(-k_1^2 A_1 + ik_1 A_2\right) = -\omega^2 \rho A\,(A_1)$$

$$GA\kappa\left(-k_1^2 B_1 + ik_1 B_2\right) = -\omega^2 \rho A\,(B_1)$$

$$GA\kappa\left(-k_1^2 C_1 + ik_1 C_2\right) = -\omega^2 \rho A\,(C_1)$$

$$GA\kappa\left(-k_1^2 D_1 + ik_1 D_2\right) = -\omega^2 \rho A\left(D_1\right)$$

So we get coefficients $[A_2...]$ in terms of $[A_1...]$ as

$$A_2 = \left[\frac{-\omega^2 \rho A + k_1^2 GA\kappa}{ik_1 GA\kappa}\right] A_1$$

$$B_2 = \left[\frac{-\omega^2 \rho A + k_2^2 GA\kappa}{ik_2 GA\kappa}\right] B_1$$

$$C_2 = \left[\frac{\omega^2 \rho A - k_1^2 GA\kappa}{ik_1 GA\kappa}\right] C_1$$

$$D_2 = \left[\frac{\omega^2 \rho A + k_2^2 GA\kappa}{ik_2 GA\kappa}\right] D_1$$

Shear force and moment equations can be written in slope forms as

$$\hat{Q} = -EI\frac{d^2\hat{o}}{dx^2} - \omega^2 \rho I \hat{o} \tag{3.19}$$

$$\hat{M} = -EI\frac{d\hat{o}}{dx} \tag{3.20}$$

The dynamic stiffness is obtained by first relating the coefficients to the nodal displacements as

$$[A_1 B_1 C_1 D_1] = \hat{\alpha}\left[\hat{y}_1, \hat{o}_1, \hat{y}_2, \hat{o}_2\right]$$

Where $[\hat{\alpha}] = \left[\hat{\beta}\right]^{-1}$ and the entries of $\left[\hat{\beta}\right]$ are

$$\hat{\beta}_{11} = 1$$

$$\hat{\beta}_{12} = 1$$

$$\hat{\beta}_{13} = 1$$

$$\hat{\beta}_{14} = 1$$

$$\hat{\beta}_{21} = \frac{GA\kappa k_1^2 - \omega^2 \rho A}{ik_1 GA\kappa}$$

$$\hat{\beta}_{22} = \frac{GA\kappa k_2^2 - \omega^2 \rho A}{ik_2 GA\kappa}$$

$$\hat{\beta}_{23} = \frac{-GA\kappa k_1^2 + \omega^2 \rho A}{ik_1 GA\kappa}$$

$$\hat{\beta}_{24} = \frac{-GA\kappa k_2^2 + \omega^2 \rho A}{ik_2 GA\kappa}$$

$$\hat{\beta}_{31} = e^{-ik_1 l}$$

$$\hat{\beta}_{32} = e^{-ik_2 l}$$

$$\hat{\beta}_{33} = e^{ik_1 l}$$

$$\hat{\beta}_{34} = e^{-ik_2 l}$$

$$\hat{\beta}_{41} = \frac{GA\kappa k_1^2 - \omega^2 \rho A}{ik_1 GA\kappa} e^{-ik_1 l}$$

$$\hat{\beta}_{42} = \frac{GA\kappa k_2^2 - \omega^2 \rho A}{ik_2 GA\kappa} e^{-ik_2 l}$$

$$\hat{\beta}_{43} = \frac{-GA\kappa k_1^2 + \omega^2 \rho A}{ik_1 GA\kappa} e^{ik_1 l}$$

$$\hat{\beta}_{44} = \frac{-GA\kappa k_2^2 - \omega^2 \rho A}{ik_2 GA\kappa} e^{ik_2 l}$$

The nodal loads are obtained by using the above shear force and moment equations (3.19) and (3.20), to give

$$\left[\hat{F}\right] = \left[\hat{K}\right]\left[\hat{d}\right] \tag{3.21}$$

Where

$$[\hat{F}]^T = [\hat{Q}_1 \hat{M}_1 ... \hat{Q}_n \hat{M}_n]$$

and

$$[\hat{d}]^T = [\hat{y}_1 \hat{\phi}_2 ... \hat{y}_n \hat{\phi}_n]$$

where n is the number of nodes. Beam, with its D.O.Fs at each node, is shown in Figure (3.2).

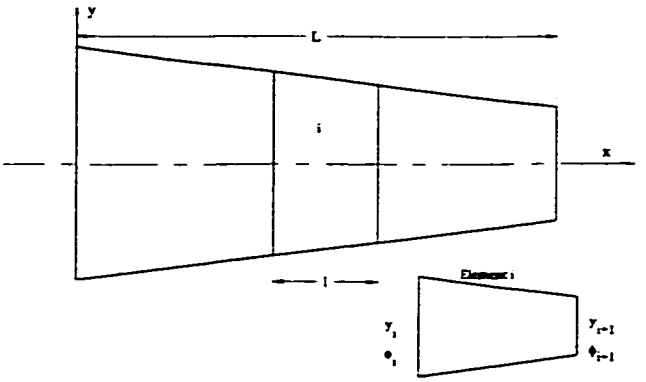

Figure 3.2: A beam and its representative element showing D.O.F used

The individual stiffness terms are

$$\begin{aligned}\hat{k}_{11} = {} & \hat{\alpha}_{11}\left[\frac{GA\kappa k_1^2-\omega^2\rho A}{GA\kappa}\right]\left[EIik_1+\frac{\rho I\omega^2}{ik_1}\right]+\\ & \hat{\alpha}_{21}\left[\frac{GA\kappa k_2^2-\omega^2\rho A}{GA\kappa}\right]\left[EIik_2+\frac{\rho I\omega^2}{ik_2}\right]+\\ & \hat{\alpha}_{31}\left[\frac{-GA\kappa k_1^2+\omega^2\rho A}{GA\kappa}\right]\left[EIik_1+\frac{\rho I\omega^2}{ik_1}\right]+\\ & \hat{\alpha}_{41}\left[\frac{-GA\kappa k_2^2+\omega^2\rho A}{GA\kappa}\right]\left[EIik_2+\frac{\rho I\omega^2}{ik_2}\right]\end{aligned} \tag{3.22}$$

$$\begin{aligned}\hat{k}_{12} = {} & \hat{\alpha}_{12}\left[\frac{GA\kappa k_1^2-\omega^2\rho A}{GA\kappa}\right]\left[EIik_1-\frac{\rho I\omega^2}{ik_1}\right]+\\ & \hat{\alpha}_{22}\left[\frac{GA\kappa k_2^2-\omega^2\rho A}{GA\kappa}\right]\left[EIik_2+\frac{\rho I\omega^2}{ik_2}\right]+\\ & \hat{\alpha}_{32}\left[\frac{-GA\kappa k_1^2+\omega^2\rho A}{GA\kappa}\right]\left[EIik_1+\frac{\rho I\omega^2}{ik_1}\right]+\\ & \hat{\alpha}_{42}\left[\frac{-GA\kappa k_2^2+\omega^2\rho A}{GA\kappa}\right]\left[EIik_2+\frac{\rho I\omega^2}{ik_2}\right]\end{aligned} \tag{3.23}$$

$$\begin{aligned}\hat{k}_{13} = {} & \hat{\alpha}_{13}\left[\frac{GA\kappa k_1^2-\omega^2\rho A}{GA\kappa}\right]\left[EIik_1+\frac{\rho I\omega^2}{ik_1}\right]+\\ & \hat{\alpha}_{23}\left[\frac{GA\kappa k_2^2-\omega^2\rho A}{GA\kappa}\right]\left[EIik_2+\frac{\rho I\omega^2}{ik_2}\right]+\\ & \hat{\alpha}_{33}\left[\frac{-GA\kappa k_1^2+\omega^2\rho A}{GA\kappa}\right]\left[EIik_1+\frac{\rho I\omega^2}{ik_1}\right]+\\ & \hat{\alpha}_{43}\left[\frac{-GA\kappa k_2^2+\omega^2\rho A}{GA\kappa}\right]\left[EIik_2+\frac{\rho I\omega^2}{ik_2}\right]\end{aligned} \tag{3.24}$$

$$\begin{aligned}\hat{k}_{14} &= \hat{\alpha}_{14}\left[\frac{GA\kappa k_1^2-\omega^2\rho A}{GA\kappa}\right]\left[EIik_1+\frac{\rho I\omega^2}{ik_1}\right]+\\ &\quad \hat{\alpha}_{24}\left[\frac{GA\kappa k_2^2-\omega^2\rho A}{GA\kappa}\right]\left[EIik_2+\frac{\rho I\omega^2}{ik_2}\right]+\\ &\quad \hat{\alpha}_{34}\left[\frac{-GA\kappa k_1^2+\omega^2\rho A}{GA\kappa}\right]\left[EIik_1+\frac{\rho I\omega^2}{ik_1}\right]+\\ &\quad \hat{\alpha}_{44}\left[\frac{-GA\kappa k_2^2+\omega^2\rho A}{GA\kappa}\right]\left[EIik_2+\frac{\rho I\omega^2}{ik_2}\right]\end{aligned} \tag{3.25}$$

$$\begin{aligned}\hat{k}_{21} &= EI\hat{\alpha}_{11}\left[\frac{-GA\kappa k_1^2+\omega^2\rho A}{GA\kappa}\right]+\\ &\quad EI\hat{\alpha}_{21}\left[\frac{-GA\kappa k_2^2+\omega^2\rho A}{GA\kappa}\right]+\\ &\quad EI\hat{\alpha}_{31}\left[\frac{-GA\kappa k_1^2+\omega^2\rho A}{GA\kappa}\right]+\\ &\quad EI\hat{\alpha}_{41}\left[\frac{-GA\kappa k_2^2+\omega^2\rho A}{GA\kappa}\right]\end{aligned} \tag{3.26}$$

$$\begin{aligned}\hat{k}_{22} &= EI\hat{\alpha}_{12}\left[\frac{-GA\kappa k_1^2+\omega^2\rho A}{GA\kappa}\right]+\\ &\quad EI\hat{\alpha}_{22}\left[\frac{-GA\kappa k_2^2+\omega^2\rho A}{GA\kappa}\right]+\\ &\quad EI\hat{\alpha}_{32}\left[\frac{-GA\kappa k_1^2+\omega^2\rho A}{GA\kappa}\right]+\\ &\quad EI\hat{\alpha}_{42}\left[\frac{-GA\kappa k_2^2+\omega^2\rho A}{GA\kappa}\right]\end{aligned} \tag{3.27}$$

$$\begin{aligned}\hat{k}_{23} &= EI\hat{\alpha}_{13}\left[\frac{-GA\kappa k_1^2+\omega^2\rho A}{GA\kappa}\right]+\\ &\quad EI\hat{\alpha}_{23}\left[\frac{-GA\kappa k_2^2+\omega^2\rho A}{GA\kappa}\right]+\\ &\quad EI\hat{\alpha}_{33}\left[\frac{-GA\kappa k_1^2+\omega^2\rho A}{GA\kappa}\right]+\\ &\quad EI\hat{\alpha}_{43}\left[\frac{-GA\kappa k_2^2+\omega^2\rho A}{GA\kappa}\right]\end{aligned} \tag{3.28}$$

$$\begin{aligned}\hat{k}_{24} &= EI\hat{\alpha}_{14}\left[\frac{-GA\kappa k_1^2+\omega^2\rho A}{GA\kappa}\right]+\\ &\quad EI\hat{\alpha}_{24}\left[\frac{-GA\kappa k_2^2+\omega^2\rho A}{GA\kappa}\right]+\\ &\quad EI\hat{\alpha}_{34}\left[\frac{-GA\kappa k_1^2+\omega^2\rho A}{GA\kappa}\right]+\\ &\quad EI\hat{\alpha}_{44}\left[\frac{-GA\kappa k_2^2+\omega^2\rho A}{GA\kappa}\right]\end{aligned} \tag{3.29}$$

$$\begin{aligned}\hat{k}_{31} &= \hat{\alpha}_{11}e^{-ik_1l}\left[\frac{GA\kappa k_1^2-\omega^2\rho A}{GA\kappa}\right]\left[EIik_1+\frac{\rho I\omega^2}{ik_1}\right]+\\ &\quad \hat{\alpha}_{21}e^{-ik_2l}\left[\frac{GA\kappa k_2^2-\omega^2\rho A}{GA\kappa}\right]\left[EIik_2+\frac{\rho I\omega^2}{ik_2}\right]+\\ &\quad \hat{\alpha}_{31}e^{ik_1l}\left[\frac{-GA\kappa k_1^2+\omega^2\rho A}{GA\kappa}\right]\left[EIik_1+\frac{\rho I\omega^2}{ik_1}\right]+\\ &\quad \hat{\alpha}_{41}e^{ik_2l}\left[\frac{-GA\kappa k_2^2+\omega^2\rho A}{GA\kappa}\right]\left[EIik_2+\frac{\rho I\omega^2}{ik_2}\right]\end{aligned} \tag{3.30}$$

$$\begin{aligned}
\hat{k}_{32} = \; & \hat{\alpha}_{12}e^{-ik_1 l}\left[\frac{GA\kappa k_1^2-\omega^2\rho A}{GA\kappa}\right]\left[EIik_1+\frac{\rho I\omega^2}{ik_1}\right]+ \\
& \hat{\alpha}_{22}e^{-ik_2 l}\left[\frac{GA\kappa k_2^2-\omega^2\rho A}{GA\kappa}\right]\left[EIik_2+\frac{\rho I\omega^2}{ik_2}\right]+ \\
& \hat{\alpha}_{32}e^{ik_1 l}\left[\frac{-GA\kappa k_1^2+\omega^2\rho A}{GA\kappa}\right]\left[EIik_1+\frac{\rho I\omega^2}{ik_1}\right]+ \\
& \hat{\alpha}_{42}e^{ik_2 l}\left[\frac{-GA\kappa k_2^2+\omega^2\rho A}{GA\kappa}\right]\left[EIik_2+\frac{\rho I\omega^2}{ik_2}\right] \qquad (3.31)
\end{aligned}$$

$$\begin{aligned}
\hat{k}_{33} = \; & \hat{\alpha}_{13}e^{-ik_1 l}\left[\frac{GA\kappa k_1^2-\omega^2\rho A}{GA\kappa}\right]\left[EIik_1+\frac{\rho I\omega^2}{ik_1}\right]+ \\
& \hat{\alpha}_{23}e^{-ik_2 l}\left[\frac{GA\kappa k_2^2-\omega^2\rho A}{GA\kappa}\right]\left[EIik_2+\frac{\rho I\omega^2}{ik_2}\right]+ \\
& \hat{\alpha}_{33}e^{ik_1 l}\left[\frac{-GA\kappa k_1^2+\omega^2\rho A}{GA\kappa}\right]\left[EIik_1+\frac{\rho I\omega^2}{ik_1}\right]+ \\
& \hat{\alpha}_{43}e^{ik_2 l}\left[\frac{-GA\kappa k_2^2+\omega^2\rho A}{GA\kappa}\right]\left[EIik_2+\frac{\rho I\omega^2}{ik_2}\right] \qquad (3.32)
\end{aligned}$$

$$\begin{aligned}
\hat{k}_{34} = \; & \hat{\alpha}_{14}e^{-ik_1 l}\left[\frac{GA\kappa k_1^2-\omega^2\rho A}{GA\kappa}\right]\left[EIik_1+\frac{\rho I\omega^2}{ik_1}\right]+ \\
& \hat{\alpha}_{24}e^{-ik_2 l}\left[\frac{GA\kappa k_2^2-\omega^2\rho A}{GA\kappa}\right]\left[EIik_2+\frac{\rho I\omega^2}{ik_2}\right]+ \\
& \hat{\alpha}_{34}e^{ik_1 l}\left[\frac{-GA\kappa k_1^2+\omega^2\rho A}{GA\kappa}\right]\left[EIik_1+\frac{\rho I\omega^2}{ik_1}\right]+ \\
& \hat{\alpha}_{44}e^{ik_2 l}\left[\frac{-GA\kappa k_2^2+\omega^2\rho A}{GA\kappa}\right]\left[EIik_2+\frac{\rho I\omega^2}{ik_2}\right] \qquad (3.33)
\end{aligned}$$

$$\begin{aligned}\hat{k}_{41} = {} & EI\hat{\alpha}_{11}e^{-ik_1 l}\left[\frac{-GA\kappa k_1^2+\omega^2\rho A}{GA\kappa}\right]+ \\ & EI\hat{\alpha}_{21}e^{-ik_2 l}\left[\frac{-GA\kappa k_2^2+\omega^2\rho A}{GA\kappa}\right]+ \\ & EI\hat{\alpha}_{31}e^{ik_1 l}\left[\frac{-GA\kappa k_1^2+\omega^2\rho A}{GA\kappa}\right]+ \\ & EI\hat{\alpha}_{41}e^{ik_2 l}\left[\frac{-GA\kappa k_2^2+\omega^2\rho A}{GA\kappa}\right]\end{aligned} \tag{3.34}$$

$$\begin{aligned}\hat{k}_{42} = {} & EI\hat{\alpha}_{12}e^{-ik_1 l}\left[\frac{-GA\kappa k_1^2+\omega^2\rho A}{GA\kappa}\right]+ \\ & EI\hat{\alpha}_{22}e^{-ik_2 l}\left[\frac{-GA\kappa k_2^2+\omega^2\rho A}{GA\kappa}\right]+ \\ & EI\hat{\alpha}_{32}e^{ik_1 l}\left[\frac{-GA\kappa k_1^2+\omega^2\rho A}{GA\kappa}\right]+ \\ & EI\hat{\alpha}_{42}e^{ik_2 l}\left[\frac{-GA\kappa k_2^2+\omega^2\rho A}{GA\kappa}\right]\end{aligned} \tag{3.35}$$

$$\begin{aligned}\hat{k}_{43} = {} & EI\hat{\alpha}_{13}e^{-ik_1 l}\left[\frac{-GA\kappa k_1^2+\omega^2\rho A}{GA\kappa}\right]+ \\ & EI\hat{\alpha}_{23}e^{-ik_2 l}\left[\frac{-GA\kappa k_2^2+\omega^2\rho A}{GA\kappa}\right]+ \\ & EI\hat{\alpha}_{33}e^{ik_1 l}\left[\frac{-GA\kappa k_1^2+\omega^2\rho A}{GA\kappa}\right]+ \\ & EI\hat{\alpha}_{43}e^{ik_2 l}\left[\frac{-GA\kappa k_2^2+\omega^2\rho A}{GA\kappa}\right]\end{aligned} \tag{3.36}$$

$$
\begin{aligned}
\hat{k}_{44} = \; & EI\hat{\alpha}_{14}e^{-ik_1 l}\left[\frac{-GA\kappa k_1^2+\omega^2\rho A}{GA\kappa}\right] + \\
& EI\hat{\alpha}_{24}e^{-ik_2 l}\left[\frac{-GA\kappa k_2^2+\omega^2\rho A}{GA\kappa}\right] + \\
& EI\hat{\alpha}_{34}e^{ik_1 l}\left[\frac{-GA\kappa k_1^2+\omega^2\rho A}{GA\kappa}\right] + \\
& EI\hat{\alpha}_{44}e^{ik_2 l}\left[\frac{-GA\kappa k_2^2+\omega^2\rho A}{GA\kappa}\right]
\end{aligned}
\tag{3.37}
$$

Chapter 4

METHOD OF SOLUTION

To get the transient response of the Timoshenko beam using Spectral Finite Element method, the input excitation signal at discrete time steps is converted into frequency domain by using Fast Fourier transformation (FFT) algorithm. The number of data points, N must be in powers of 2. Then power spectrum of the signal is obtained. The sampling rate, Δt must be in accordance with nyquist frequency of the signal. Frequency step is obtained by using:

$$\Delta f = \frac{1}{N \Delta t} \tag{4.1}$$

From the power spectrum, the signal is band-limited between minimum frequency , f_{min} and the maximum frequency , f_{max}. The beam is discretized into a number of elements.

Starting from the minimum frequency, assembled real dynamic stiffness matrix and

assembled load vector in frequency domain are obtained by the well-established Finite Element method to get:

$$\left[\hat{F}\right] = \left[\hat{K}\right]\left[\hat{d}\right] \tag{4.2}$$

or

$$[\hat{d}] = [\hat{K}]^{-1}[\hat{F}] \tag{4.3}$$

After applying the boundary conditions to equation (4.2), $\left[\hat{K}\right]$ is inverted by Gauss-reduction method. Thus response is obtained at f_{min}. The procedure is repeated for other frequencies upto f_{max}. Then the displacement vector, $[\hat{d}]$ is obtained at the desired node. This frequency dependant response is reconstructed into time domain by using Inverse Fourier transformation (IFFT). All this method is shown schematically in Figure (4.1) In the present study, to improve the stability of the method, damping is induced by writing the wave number, κ in the form

$$\kappa = \kappa_0(1 - i\eta) \tag{4.4}$$

Where κ_0 is the undamped value. Unless specified, η will be taken as 0.025.

4.1 INITIAL AND BOUNDARY CONDITIONS

Displacements and velocities are zero initially. Boundary conditions to be imposed are quite similar to those of the conventional element and they are imposed in the usual way. The different boundary conditions that can be applied are outlined here.

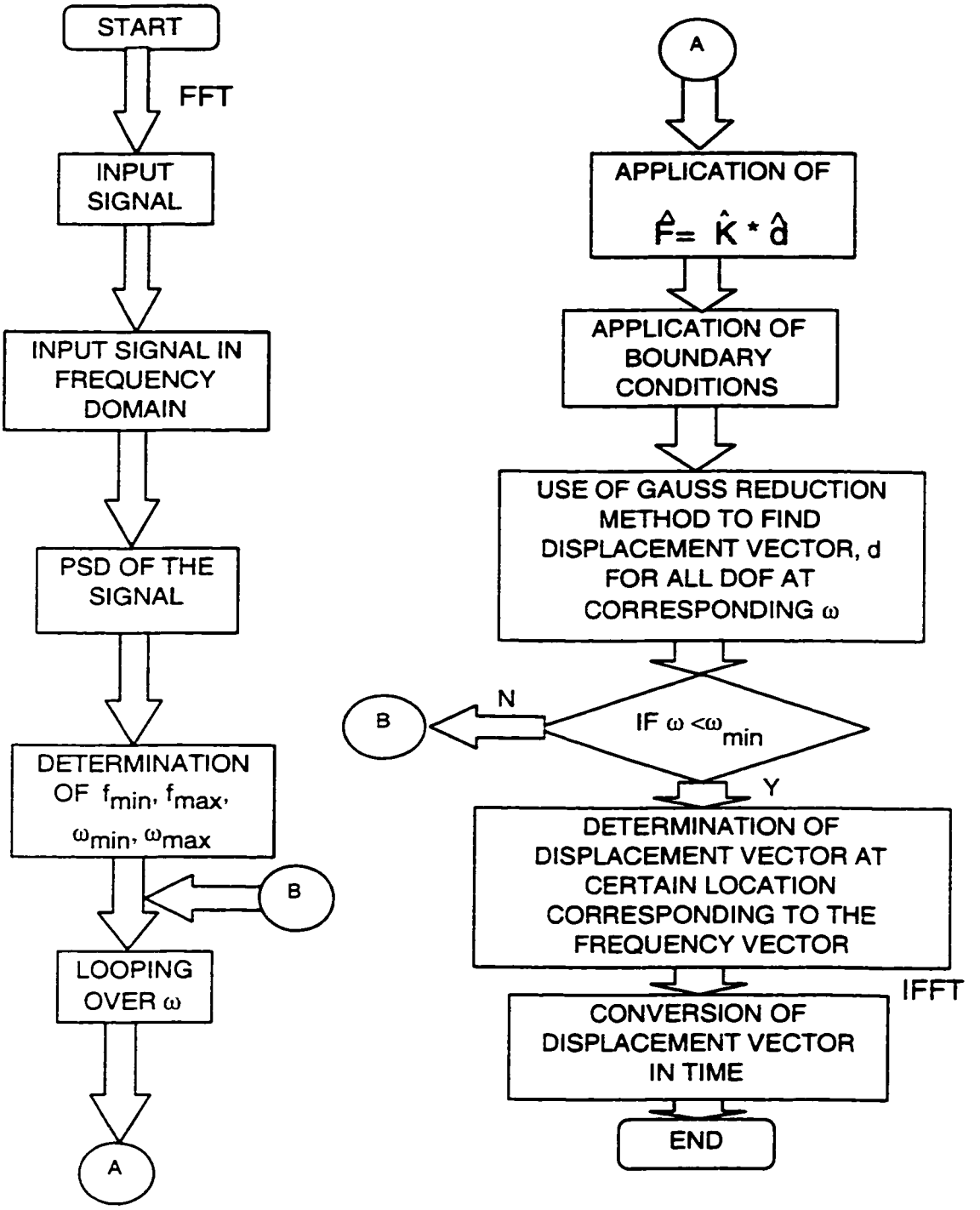

Figure 4.1: Method of solution flow chart

4.1.1 FIXED END

At fixed end ($x = 0$), displacement and bending slope are zero for all values of frequency.

$$\hat{y}(0,\omega) = \hat{\phi}(0,\omega) = 0 \tag{4.5}$$

4.1.2 HINGED END

At hinged end ($x = 0$), displacement and bending moment is zero at all frequencies.

$$\hat{y}(0,\omega) = \frac{d\hat{\phi}(0,\omega)}{dx} = 0 \tag{4.6}$$

Degrees of freedom (D.O.F) in our model are not enough to handel the zero bending moment at hinged end.

4.1.3 FREE END

At free end ($x = l$), the bending moment is zero at all frequencies.

$$\frac{d\hat{\phi}(l,\omega)}{dx} = 0 \tag{4.7}$$

Again, the D.O.F are not enough in our model to take care of this boundary condition.

4.1.4 THROW-OFF ELEMENT

There is an additional condition that is unique to wave propagation. It corresponds to when the element extends to infinity, that is, the element behaves as a throw-off

beam in that it is a conduit for energy out of the system. This boundary condition is very useful when the time of interest is short and the structure is large. Then the structure can be partitioned into local and remote parts, and the connections replaced with throw-off element that conduct energy out of the local substructure. This boundary conditioned is discussed in detail later.

4.2 THICKNESS VARIATIONS

For the sake of simplicity and demonstration of our model, the profiles taken for the thickness variation of the beams are linear and parabolic, as shown in Figure (4.2). Eight different schemes of variation are used and the thickness is varied only in x-direction. In all the types of thickness variation, its total mass remains unchanged.

The different types of the thickness variation are as follows:

1. Linear/parabolic increasing thickness

$$h_x = h_{max}\left(1 - TR\left(1 - \frac{x}{l}\right)^n\right) \tag{4.8}$$

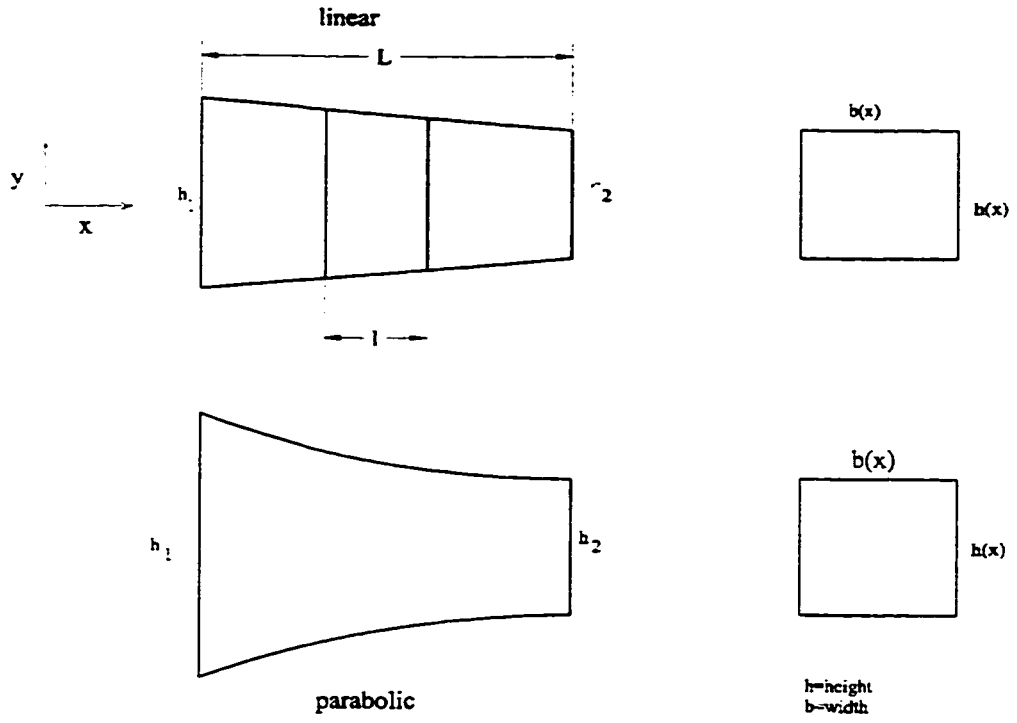

Figure 4.2: Types of thickness variations used in beam

2. Linear/parabolic decreasing thickness

$$h_x = h_{max}\left(1 - TR\left(\frac{x}{l}\right)^n\right) \tag{4.9}$$

3. Linear/parabolic decreasing-increasing thickness

$$h_x = h_{max}\left(TR\left(1 - \left|1 - 2\frac{x}{l}\right|\right)^n\right) \tag{4.10}$$

4. Linear/parabolic increasing-decreasing thickness

$$h_x = h_{max}\left(1 - TR\left|1 - 2\frac{x}{l}\right|^n\right) \tag{4.11}$$

Here h_x=thickness of the beam at a distance x

TR=taper ratio defined by $TR = 1 - \frac{h_{min}}{h_{max}}$

n=parameter, $n = 1$ for linear and $n = 2$ for parabolic variation

h_{min}=minimum thickness of the beam

h_{max}=maximum thickness of the beam

For constant thickness $TR = 0$. Unless specified, variation will be considered only in thickness.

A beam with linear variation in width is also studied in the present work. So the above variations can be employed in width also, using $n = 1$ (for linear variation).

Chapter 5

RESULTS AND DISCUSSION

In the present study Timoshenko beams are studied for different linear and parabolic thickness variations. Also different boundary conditions are considered. The studied beams are assumed to be made of steel with the properties $E = 2.068 * 10^{11}$ N/m^2 and $\rho = 7830$ kg/m^3

5.1 EXCITATION FORCE

To excite the beam, a $50MHz$ sinusoidal tone burst signal modulated temporally is used. The modulation is used to limit the bandwidth of the signal. This excitation force and its PSD are shown in Figure (5.1). The minimum frequency, f_{min} is 50 kHz and maximum frequency, f_{max} is 80 kHz.

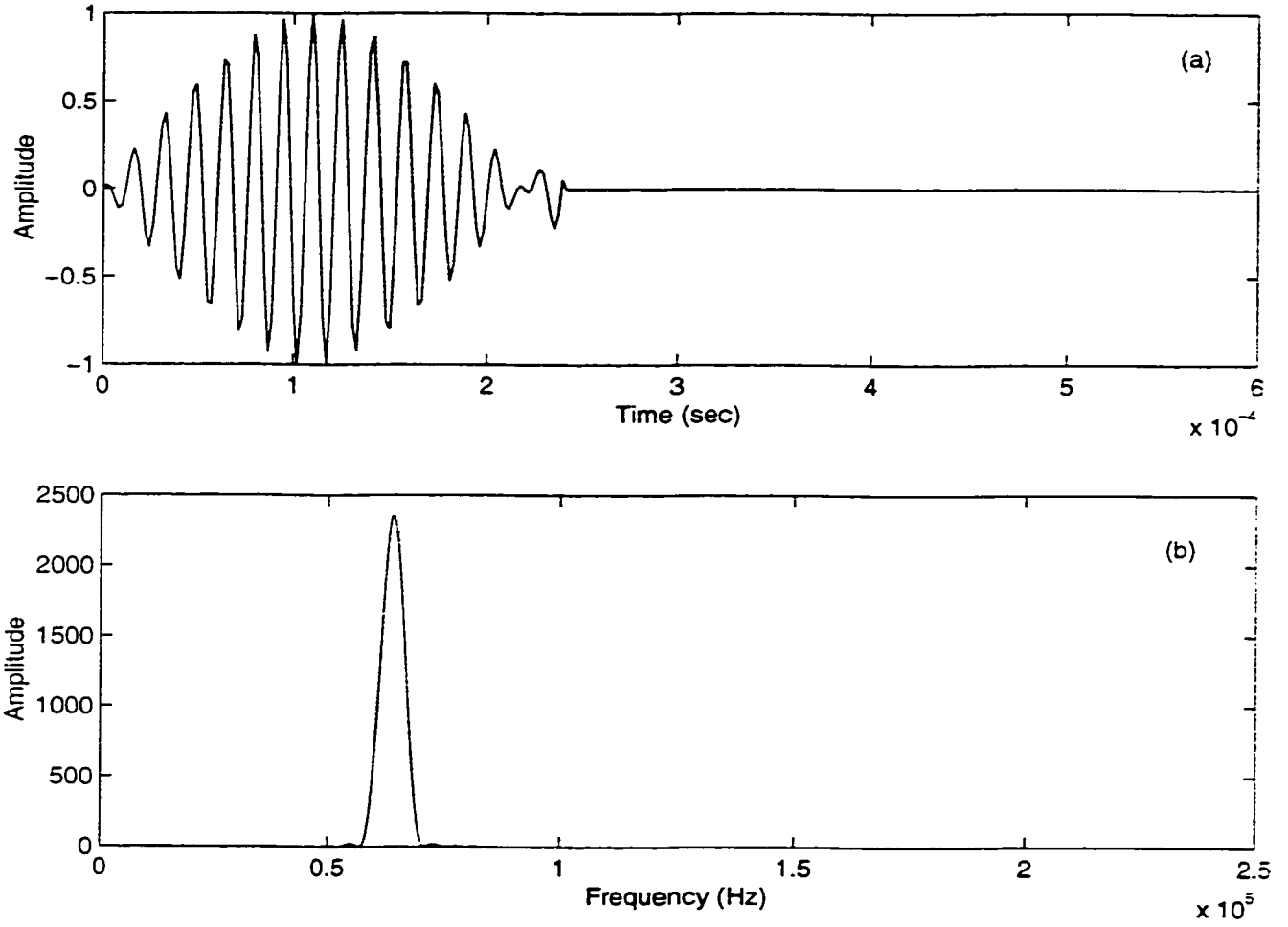

Figure 5.1: Excitation force and its Power Spectrum Density

5.2 VALIDATION OF SPECTRAL FINITE ELEMENT METHOD

For the best of our knowledge, no analytical solution is available for uniform thickness Timoshenko beams, so the present method is compared with existing analytical solution for uniform thickness Euler beams.Figure (5.2) shows the comparison of analytical wave solution with spectral Euler cantilever beam of uniform thickness. The response of the beam is demonstrated at the mid of the beam while the force is applied at the other end. The result shows excellent agreement with the analytical solution. For the spectral Euler beam here, only two elements are used to find the converged response at the node. The difference in displacement amplitude from the analytical solution may be because of the numerical methodology adopted here. However, the agreement in arrival time of the pulse is clearly demonstrated.

5.3 COMPARISON BETWEEN TIMOSHENKO AND EULER MODELS

In the formulation of Timoshenko beam two terms i.e; rotary inertia and shear deformation are included. Figure (5.3) shows the comparison between Timo-

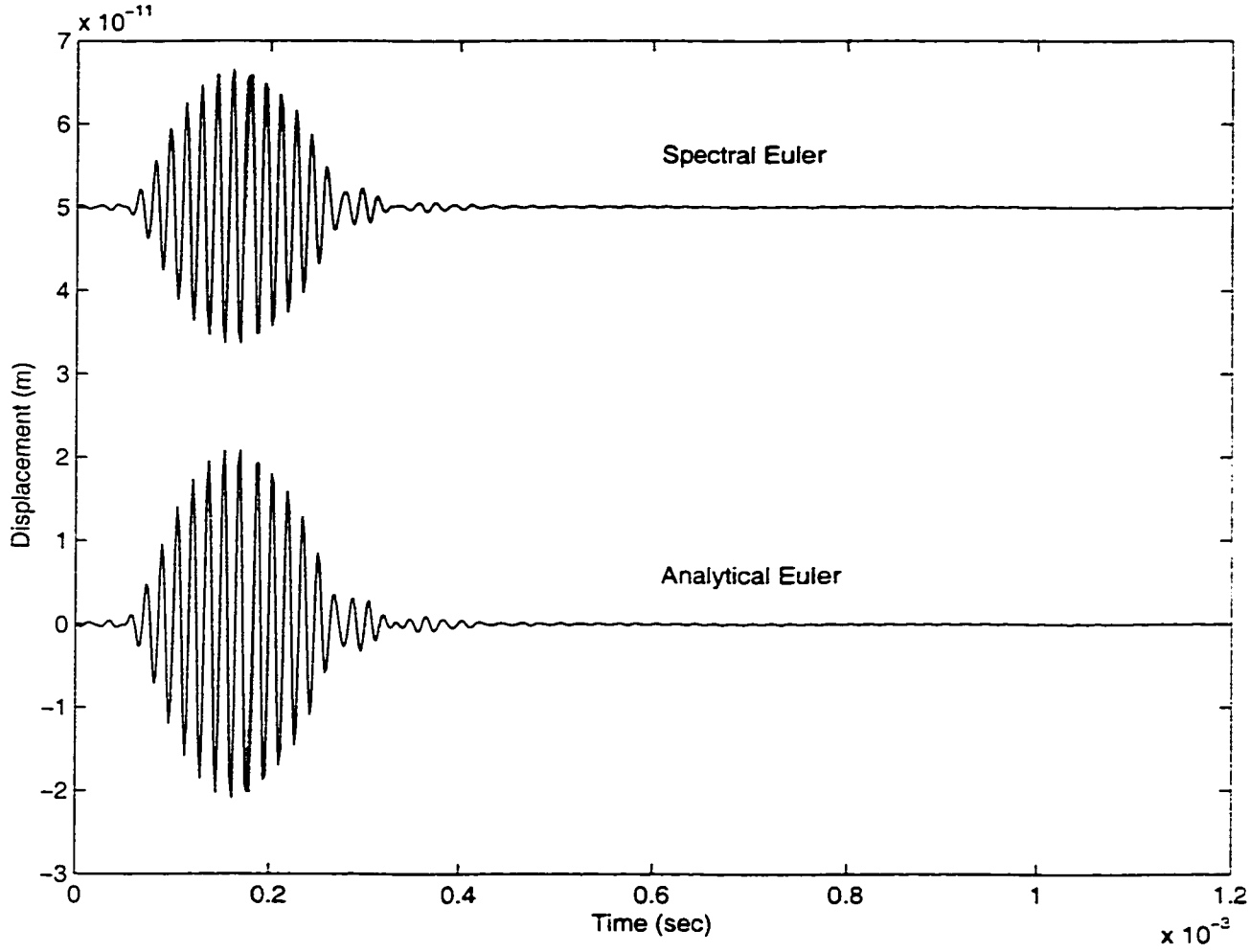

Figure 5.2: Comparison between Analytical and Spectral Euler beam

shenko and Euler beam solutions for constant thickness at the mid of the beam. with one end clamped and the other free. It is clear from this figure that the Timoshenko beam sees the travelling wave a bit later. This is because of decreased stiffness in Timoshenko beams as compared to that in Euler beams. which in turn decreases the group speed. It is also evident from the figure that there is one dominant travelling mode. This is due to the fact that the applied force contains prominent frequency range well above the cutoff frequency of the second mode. The second mode seems to be hidden at the front of the first dominant mode. It is also clear from the figure that the effect of wave is sustained a little longer in Timoshenko beam than in Euler beam because of overlapping of two modes due to the reflection from the boundaries.

5.4 LINEARLY VARYING TIMOSHENKO BEAM

Timoshenko beam thickness is linearly varied and the response is obtained for cantilever and other boundary conditions. The dimensions of the beam. are selected to make the cut off frequency well below the lowest dominant frequency in the input signal, thus allowing both modes to propagate. The taper ratios (TR) used in this analysis are 0.14, 0.29, 0.43 and 0.57. Three

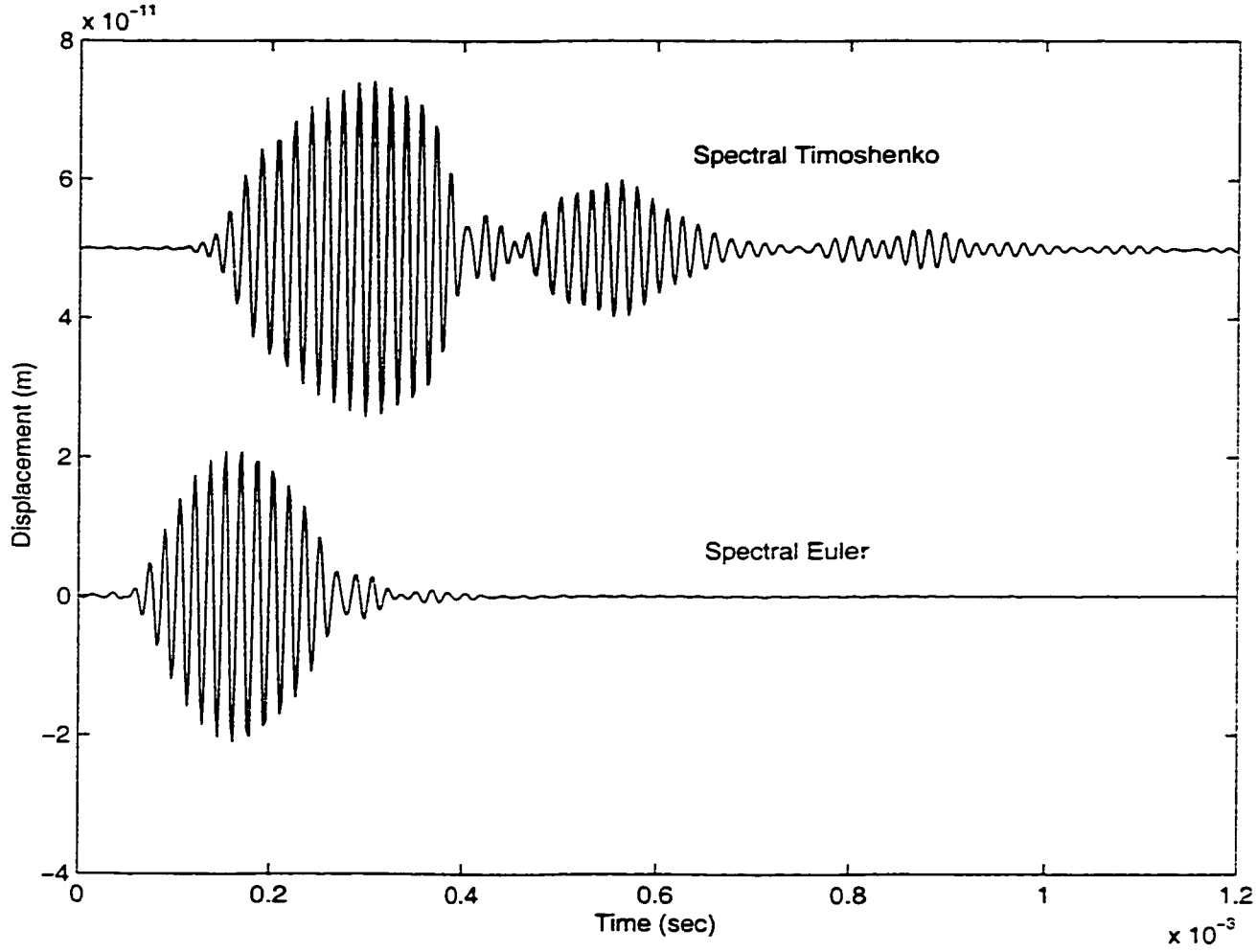

Figure 5.3: Comparison between Spectral Euler and Timoshenko beam

boundary conditions employed here are cantilever, simply supported and fixed-hinged. All the boundary conditions used are shown in Figure (5.4). It is worthnoting that no previous work is available to compare the results with. Even if we ignore rotary inertia and use infinitely high shear deformation term, the results can't be compared with Euler beam of the same specifications and under the same loading. However at high frequencies Euler beam theory fails to predict the results correctly.

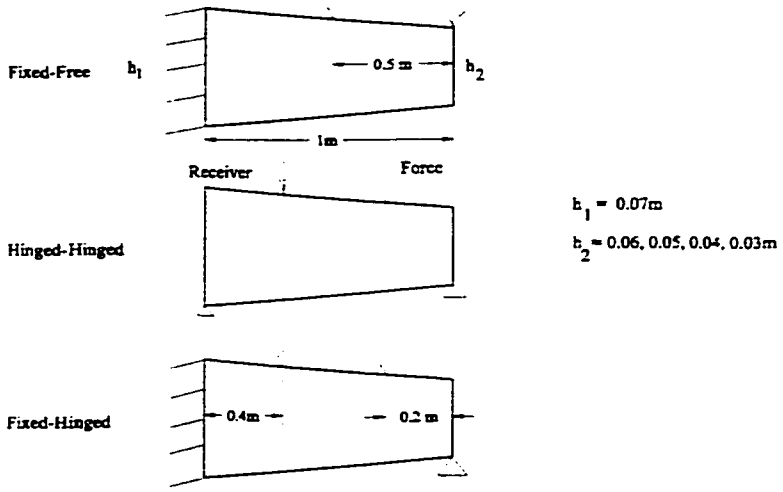

Figure 5.4: Different types of boundary conditions used

5.4.1 CANTILEVER TIMOSHENKO BEAM

Figure (5.5) shows the response of a cantilever Timoshenko beam at the mid of beam while load applied at the end. The number of elements used are 40. However if we go away from the load end while the load is applied at

the end, then more number of elements are needed for convergence. So to capture the response at 8 equally spaced locations on $1m$ long beam, we used 64 elements. As shown in Figure (5.6) and Figure(5.7) it is clear that as we go away from the load end there is distortion in the response pulse due to dispersion. From $x = 1$ m to $x = 0.625$ m only first mode was prominent with no distinct reflection. As we go to the left the second mode and the reflection start showing their presence. It is interesting that at $x = 0.125$ m which is very close to the fixed end, two modes overlap and almost died out. The group speed, c_g of the first mode is about 3125 m/s. So the reflection from the fixed end must take time $0.48 * 10^{-3}$ s to reach the mid of the beam. But reflection reaches there a bit later which indicates the reduction in group speed on reflection from fixed boundary. This needs much more investigation.

In Figure (5.8) the response of the midpoint is shown under the same loading for $TR = 0.29$. The number of elements needed for convergence is 90. The amplitude of response has increased here as compared to the previous case. The response dies out a bit later than the previous case. Only first propagating mode is predominant here while the reflections are not distinguishable. Figure (5.8) shows the response of same point for $TR = 0.43$. Here two modes seem to overlap and the response stays more longer than for the previous taper ratio. The number of elements used are 100. The amplitude of response falls

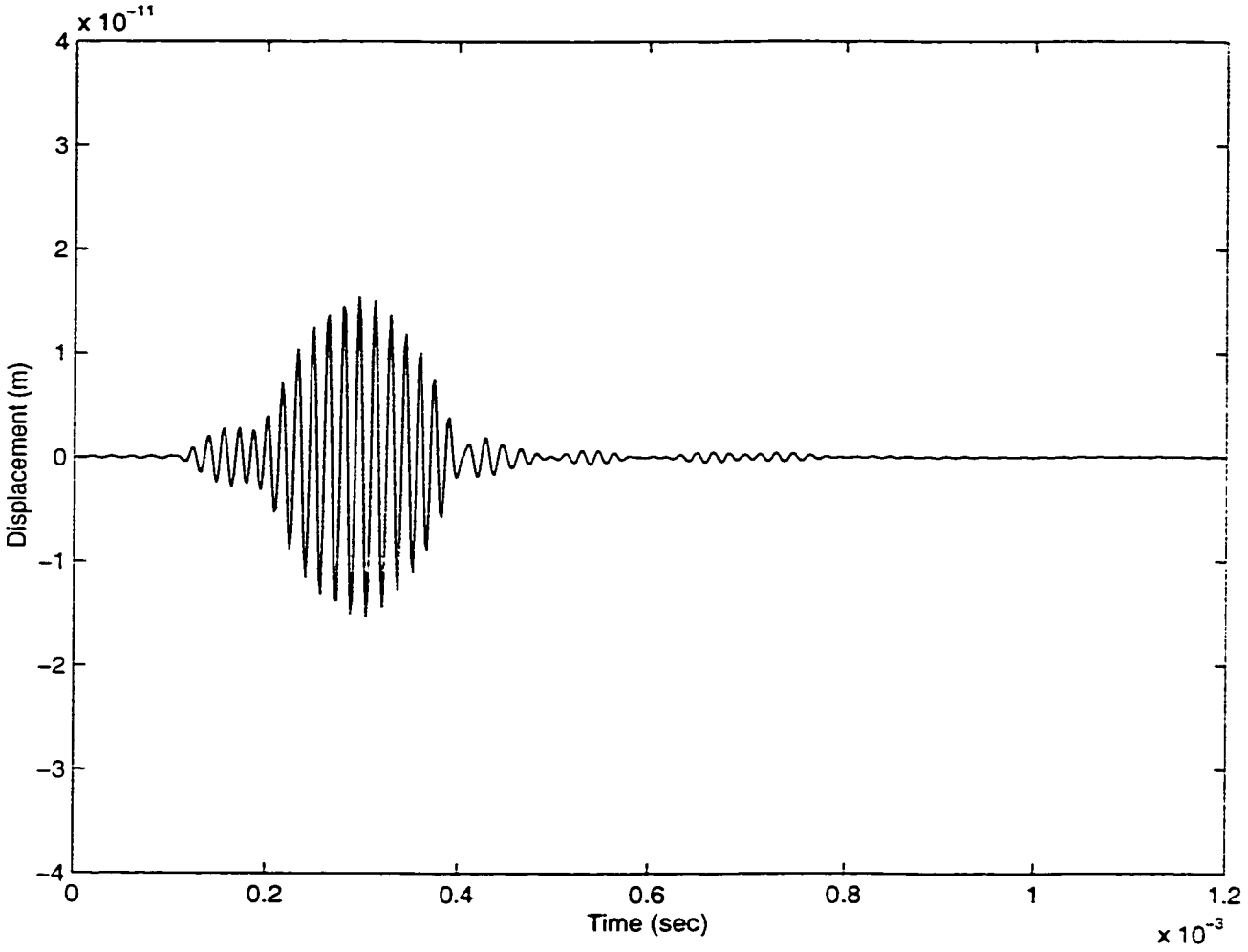

Figure 5.5: Response at the mid of linearly varying cantilever Timoshenko beam for $TR = 0.14$

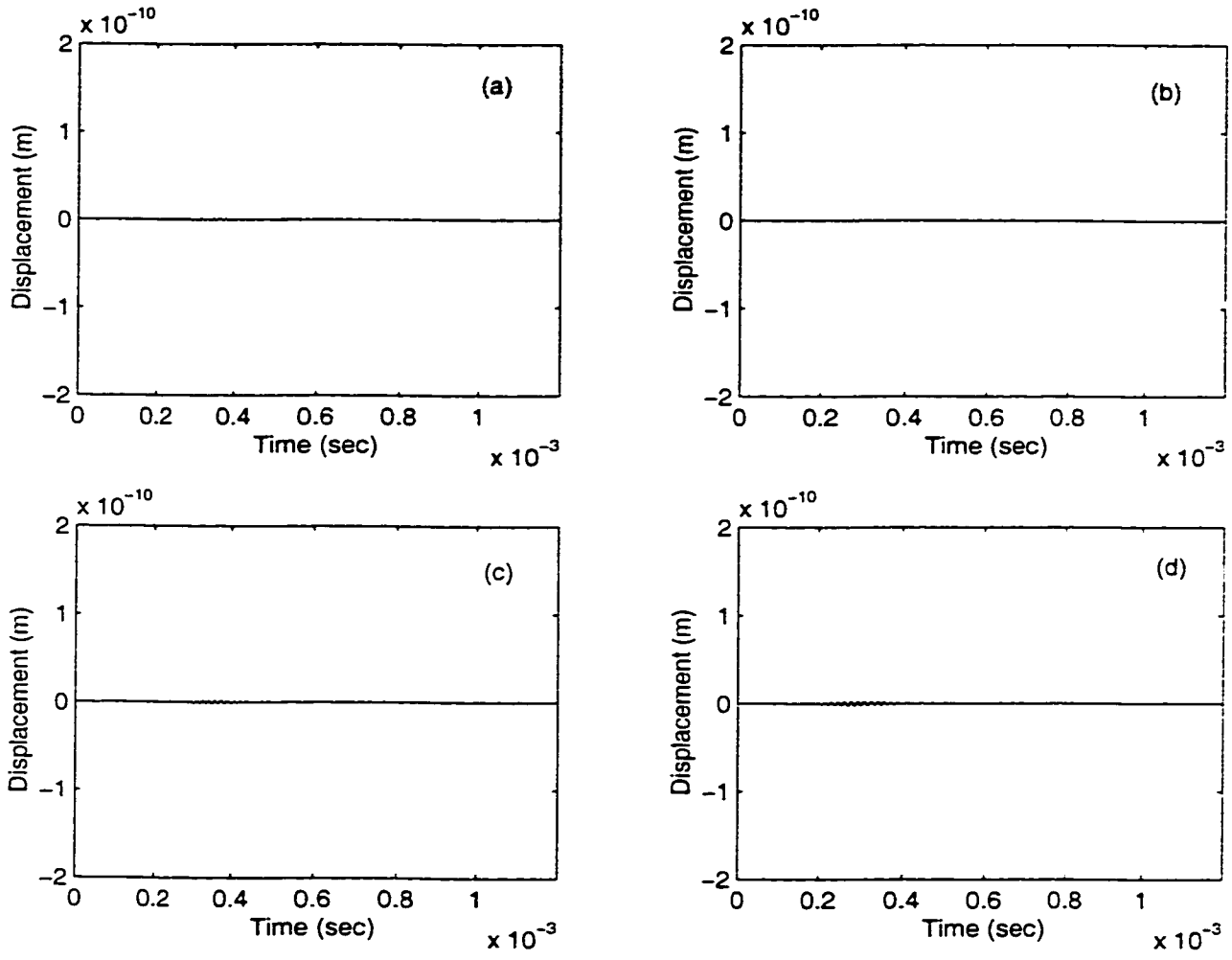

Figure 5.6: Response of linearly varying cantilever Timoshenko beam for $TR = 0.14$ at x= (a) $0.125m$ (b) $0.25m$ (c) $0.375m$ (d) $0.5m$

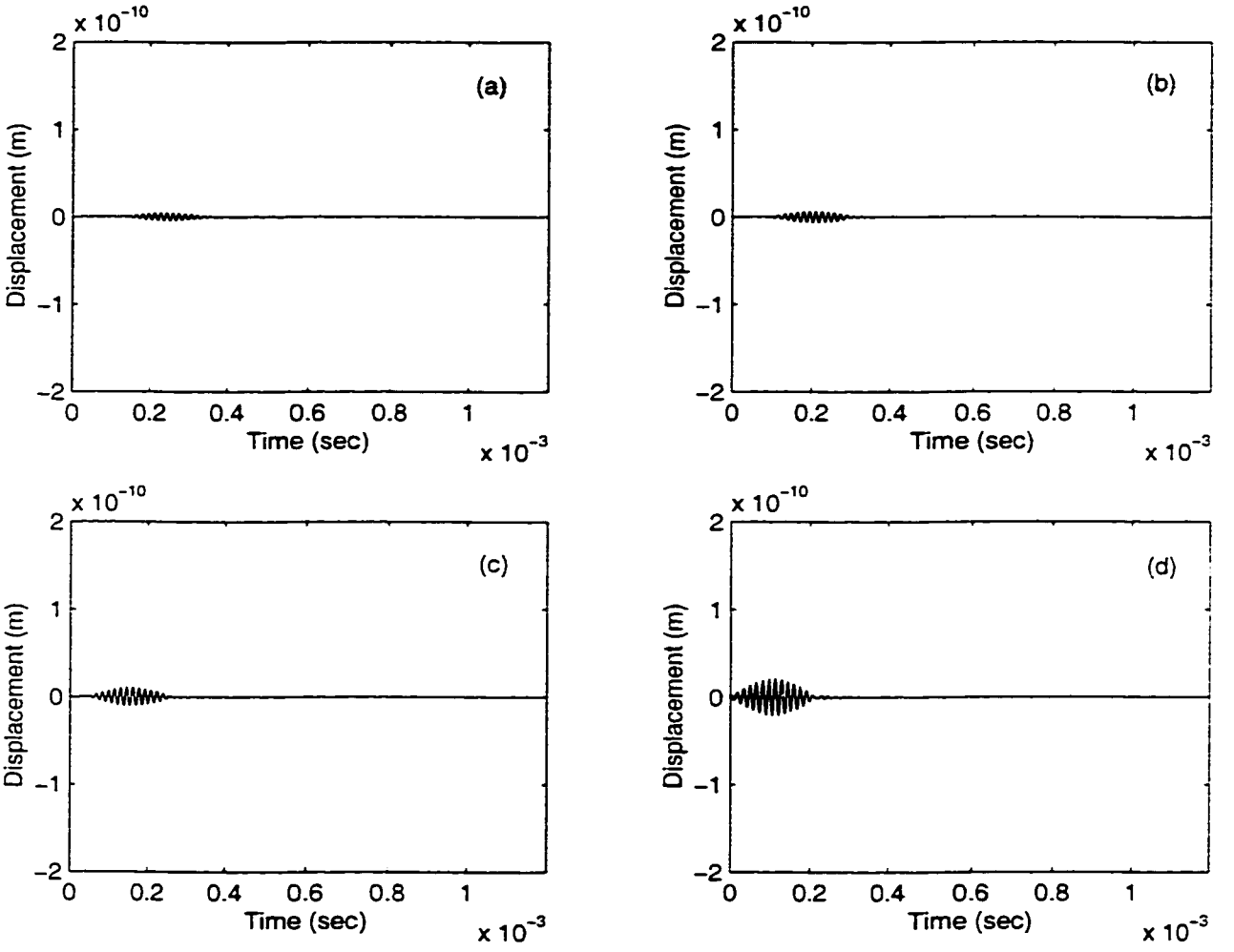

Figure 5.7: Response of linearly varying cantilever Timoshenko beam for $TR = 0.14$ at x= (a) $0.625m$ (b) $0.75m$ (c) $0.875m$ (d) $1m$

a bit than second taper ratio and also the reflection is a bit distinct. For the $TR = 0.57$ shown in Figure (5.9) the number of elements used are 110. Here predominantly only first mode is present and is clearly overlapped with second mode. The amplitude once again increased and is maximum than for other taper ratios. The modes are investigated and studies with more insight later.

5.4.2 SIMPLY SUPPORTED TIMOSHENKO BEAM

For simply supported beam the load is applied at 0.2 m from the right support and the response is captured at 0.4m from the left support. For $TR = 0.14$ the number of elements used are 50. As shown in Figure (5.10) two distinct pulses are propagating: a mode and its reflection. Like the cantilever beam the dominant mode (first mode) is slower than the second mode which is not clearly distinguishable from first mode. For $TR = 0.29$, as shown in Figure (5.10), the response amplitude is increased and the time of stay lengthens a little. The number of elements used are 60. The dominant mode (first mode) becomes much more dominant and the second mode starts showing its presence ahead of first mode and reflection is clearly distinct from the first mode. For $TR = 0.43$, as shown in Figure (5.11) the number of elements used are 80. Here unlike the cantilever case, the response amplitude increases than that for $TR = 0.29$. But still the duration of the observed wave is little more greater

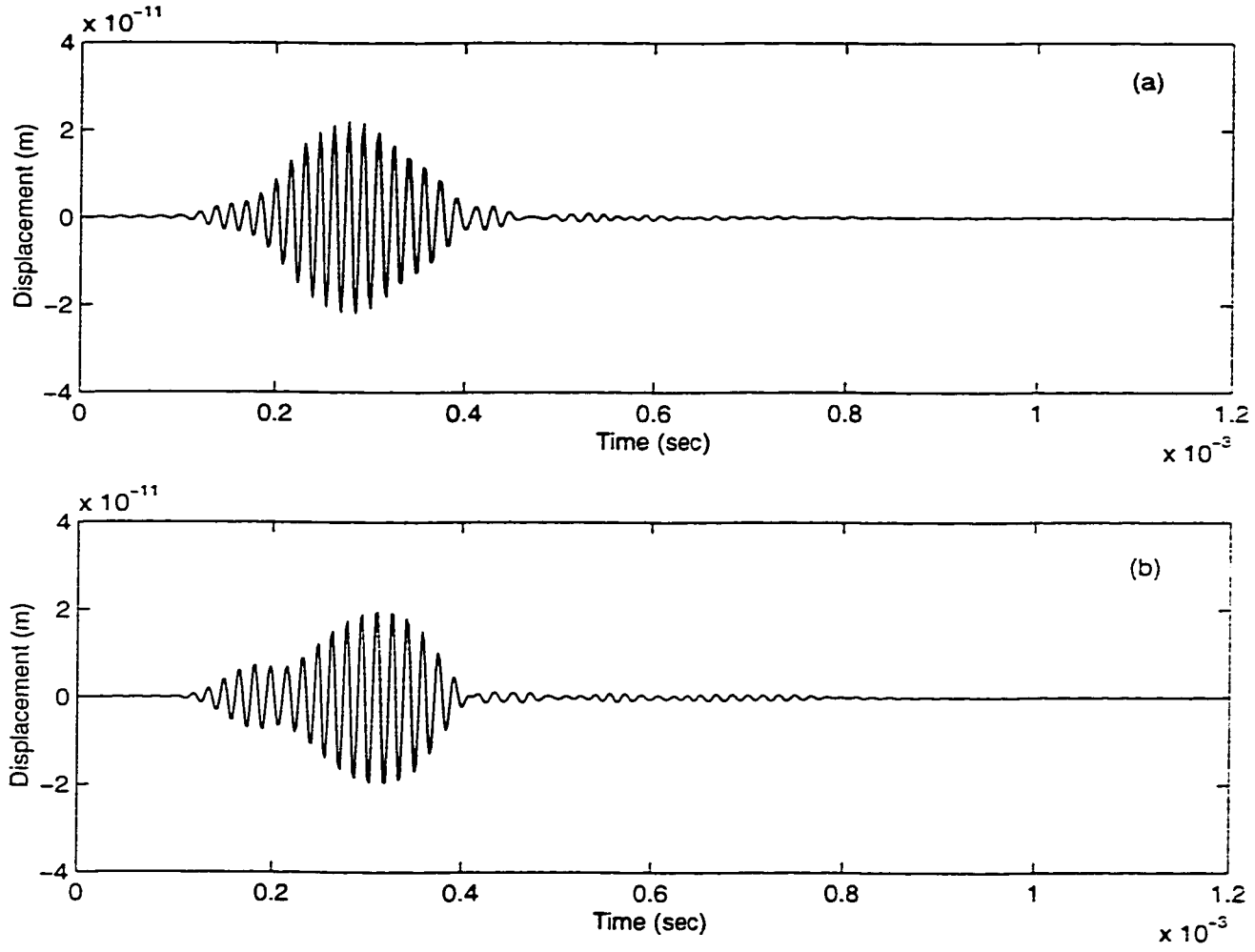

Figure 5.8: Response at the mid of linearly varying cantilever Timoshenko beam for (a) $TR = 0.29$ (b) $TR = 0.43$

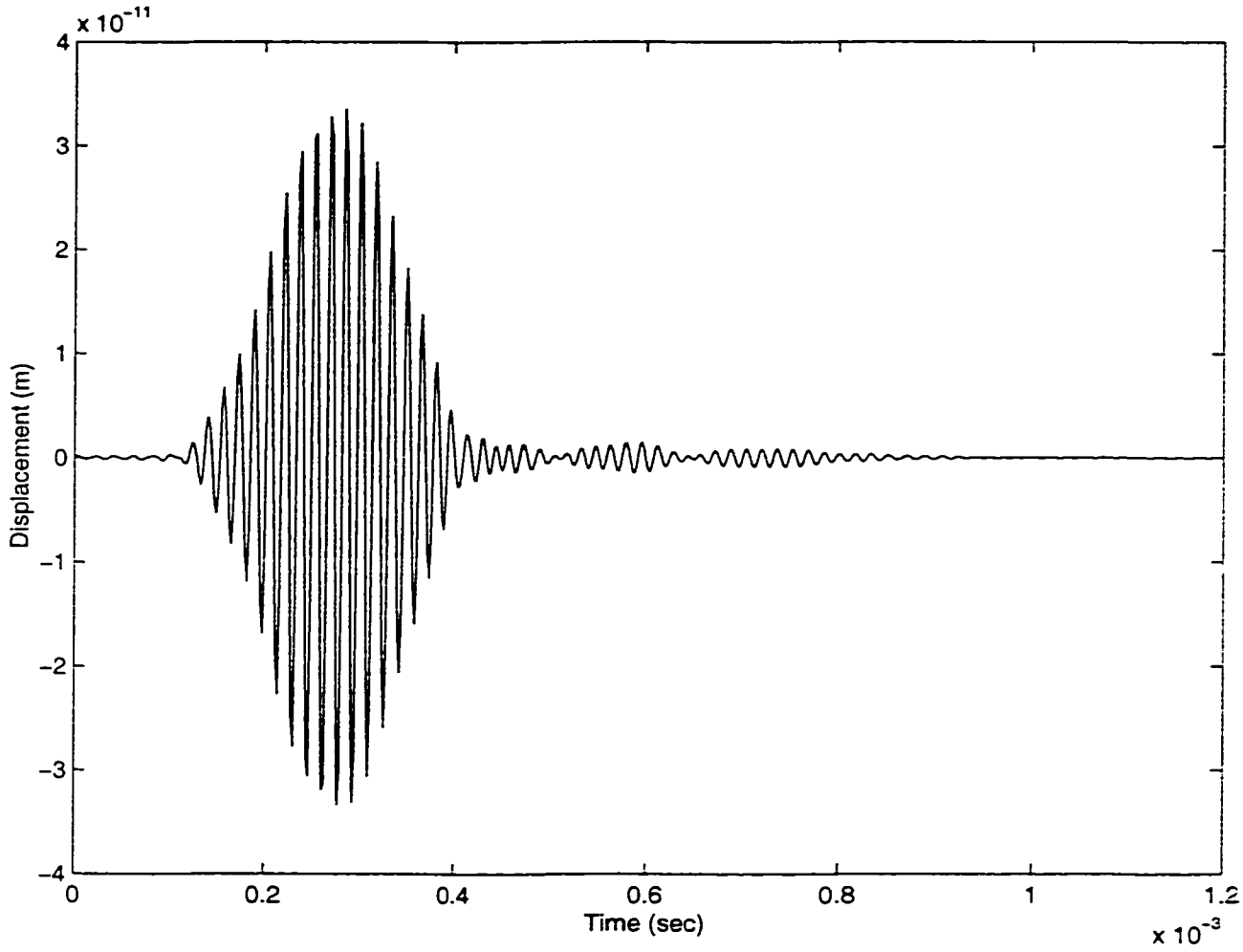

Figure 5.9: Response at the mid of linearly varying cantilever Timoshenko beam for $TR = 0.57$

than the previous taper ratios. Here the two modes are distinct eventhough the second mode seems to be weak. But reflection starts overlapping with the first mode. In $TR = 0.57$ case shown in Figure (5.11), the amplitude of response is increased more and stays more longer. Here number of elements used are 100. Only the first mode seems to be propagating while the reflection can be seen at the tail of this dominant mode.

5.4.3 FIXED-HINGED TIMOSHENKO BEAM

In this case, the load and receiver are at the same locations as they were in simply supported case. The response of the beam is shown in Figure (5.12) for only $TR = 0.57$, where 100 elements are used. The amplitude of the response in the dominant mode is little greater than its counterpart simply supported case. As it can be seen, the second mode doesn't appear. The group velocity of the first mode seems to be approximately the same as that for the simply supported beam.

5.5 PARABOLIC THICKNESS VARIATION

100 elements are used here. The thickness at the fixed end is 0.07 m and at the force end is 0.03 m. In contrast to the linearly varying cantilever beam, the response here is much reduced and two modes are visible and distinguishable

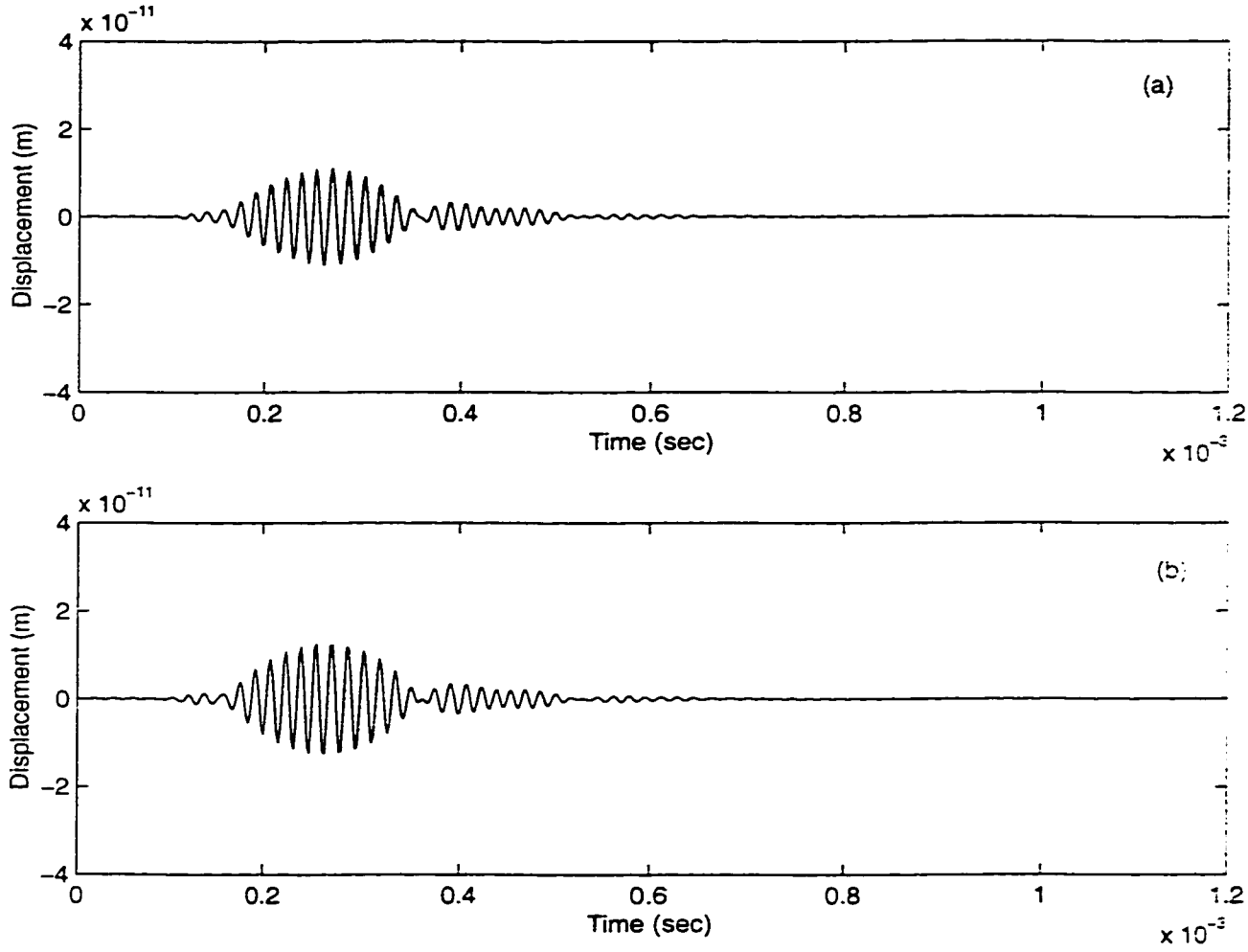

Figure 5.10: Response at the mid of linearly varying simply supported Timoshenko beam for (a) $TR = 0.14$ (b) $TR = 0.29$

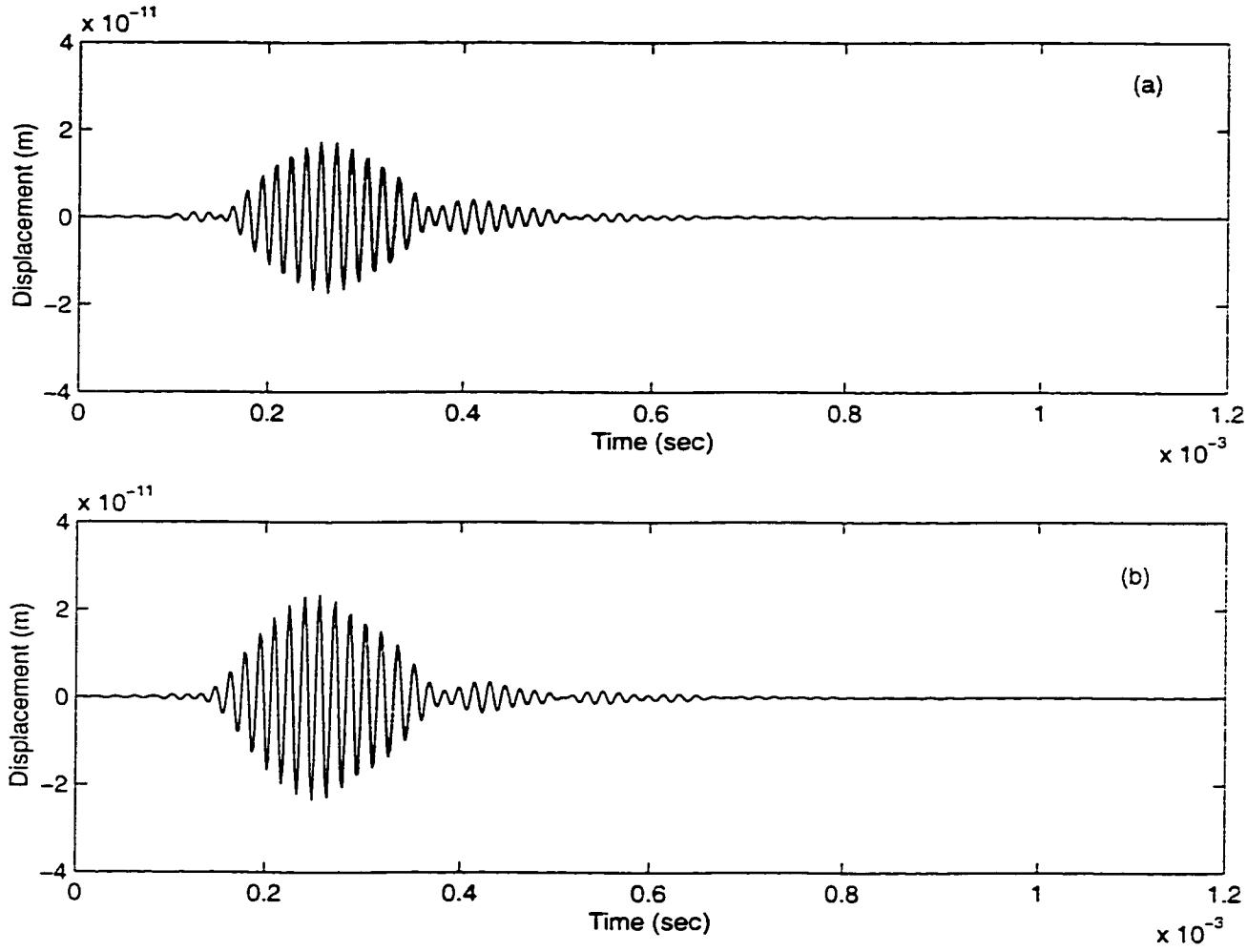

Figure 5.11: Response at the mid of linearly varying simply supported Timoshenko beam for (a) $TR = 0.43$ (b) $TR = 0.57$

alongwith reflections as shown in Figure (5.12). The second mode is faster than the first mode and it is clearly ahead of it. Group speed of first mode is 2272.7 m/s and that of second mode observed here is 7142.8 m/s. Moreover, it seems that the group velocity of the first mode for the parabolic variation is less than that for the linear variation case.

5.6 THROW OFF ELEMENT

The throw off element acts as conduit of energy, the throw-off element used here is of constant thickness and applied to cantilever beam. Figure (5.13) shows the response of constant thickness cantilever beam at various locations and Figure (5.14) shows the responses at same locations when right handed throw off element is used. Since there is no reflection from the right end in throw off case, the general solution for this element becomes:

$$\hat{y} = A_1 e^{-ik_1 x} + A_2 e^{-ik_2 x}$$

It's clear from Figure (5.14) that the damping in the beam has increased in the system by the introduction of throw off element. If we compare these results with those of beams without throw off element, one can notice the disappearance of the right end boundary. The elements used in this case

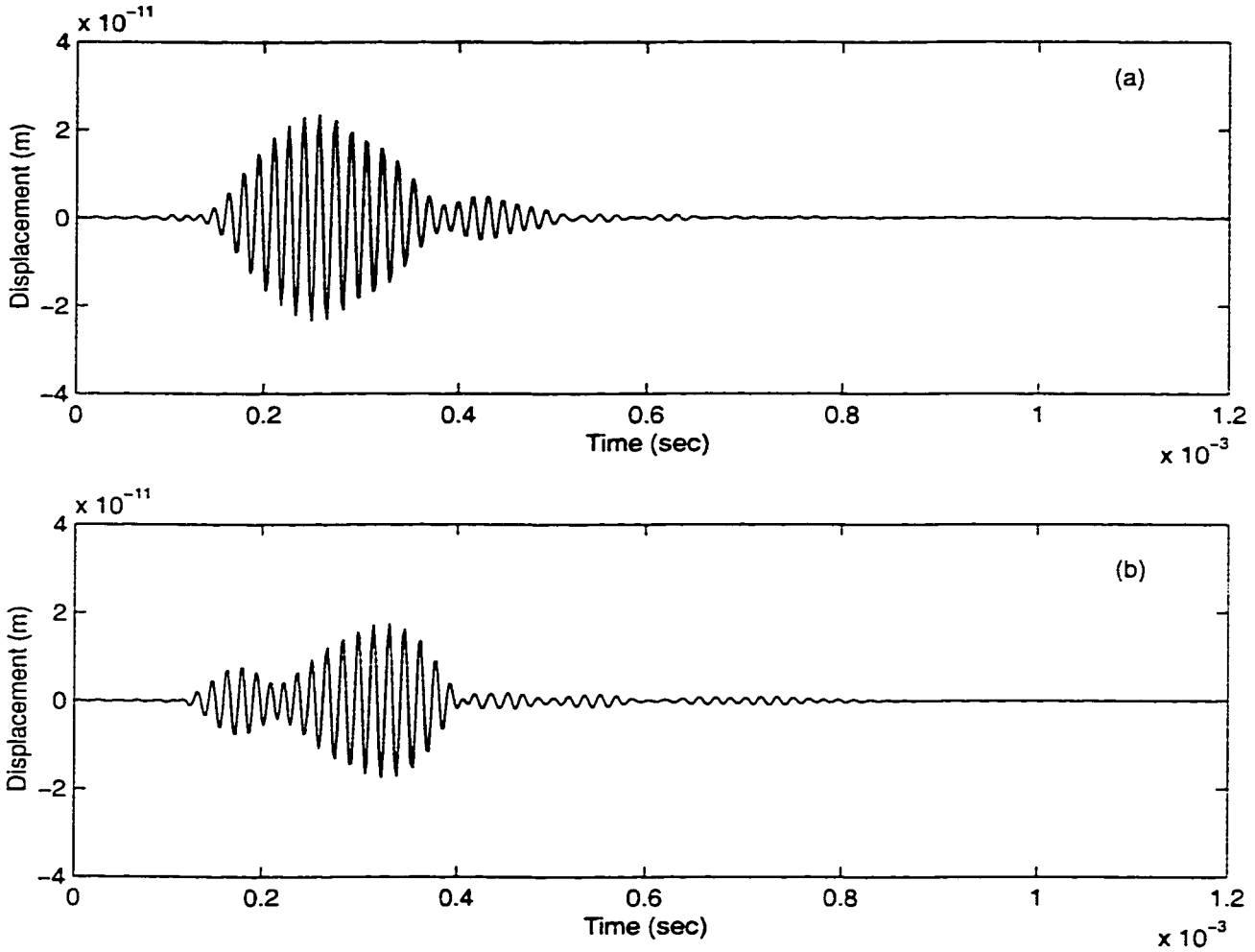

Figure 5.12: (a)Response at the mid of linearly varying clamped-Hinged Timoshenko beam for $TR = 0.57$ (b)Response at the mid of parabolically varying cantilever Timoshenko beam for $TR = 0.57$

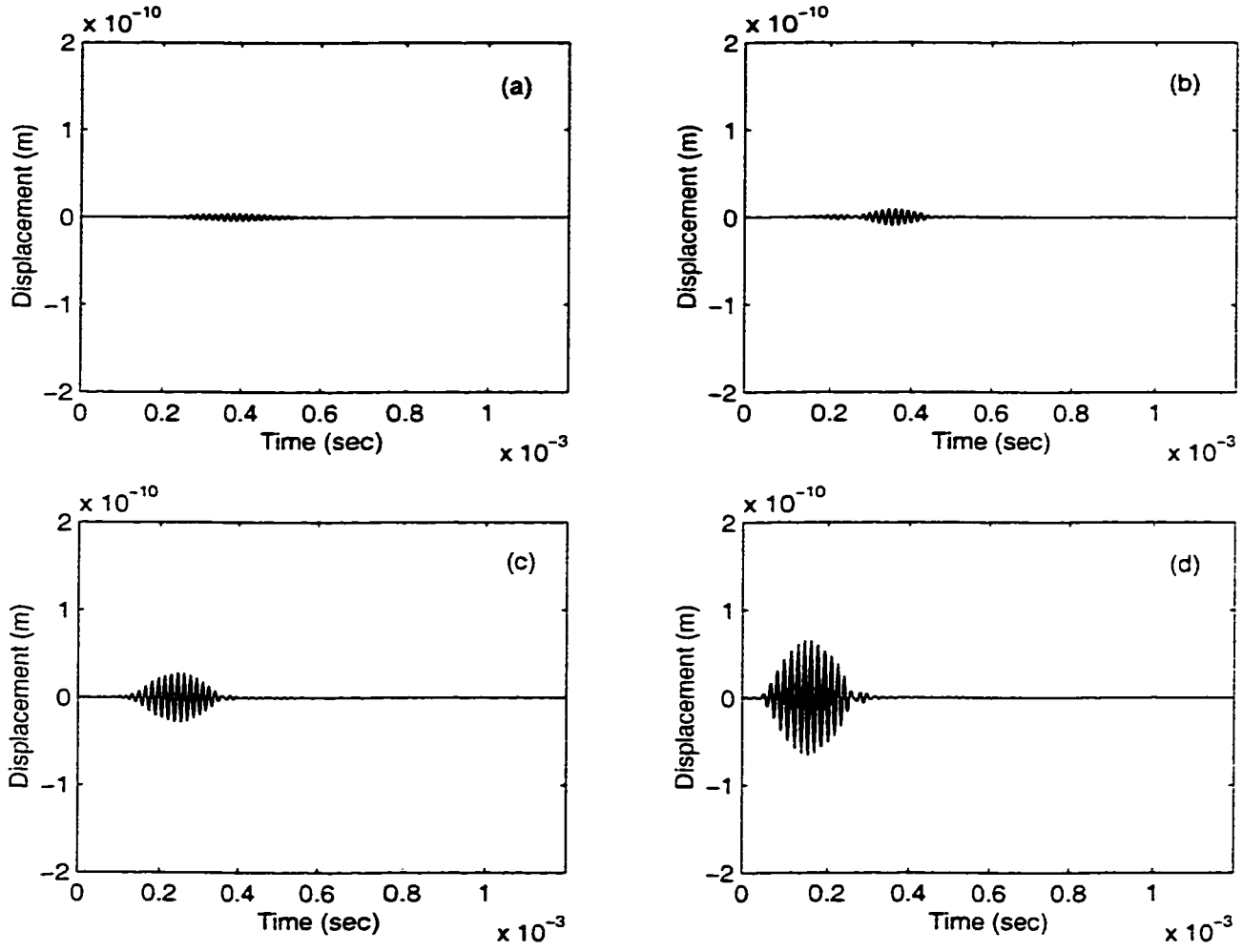

Figure 5.13: Response of constant thickness (0.03 m) cantilever Timoshenko beam at x= (a) $0.125m$ (b) $0.375m$ (c) $0.625m$ (d) $0.875m$

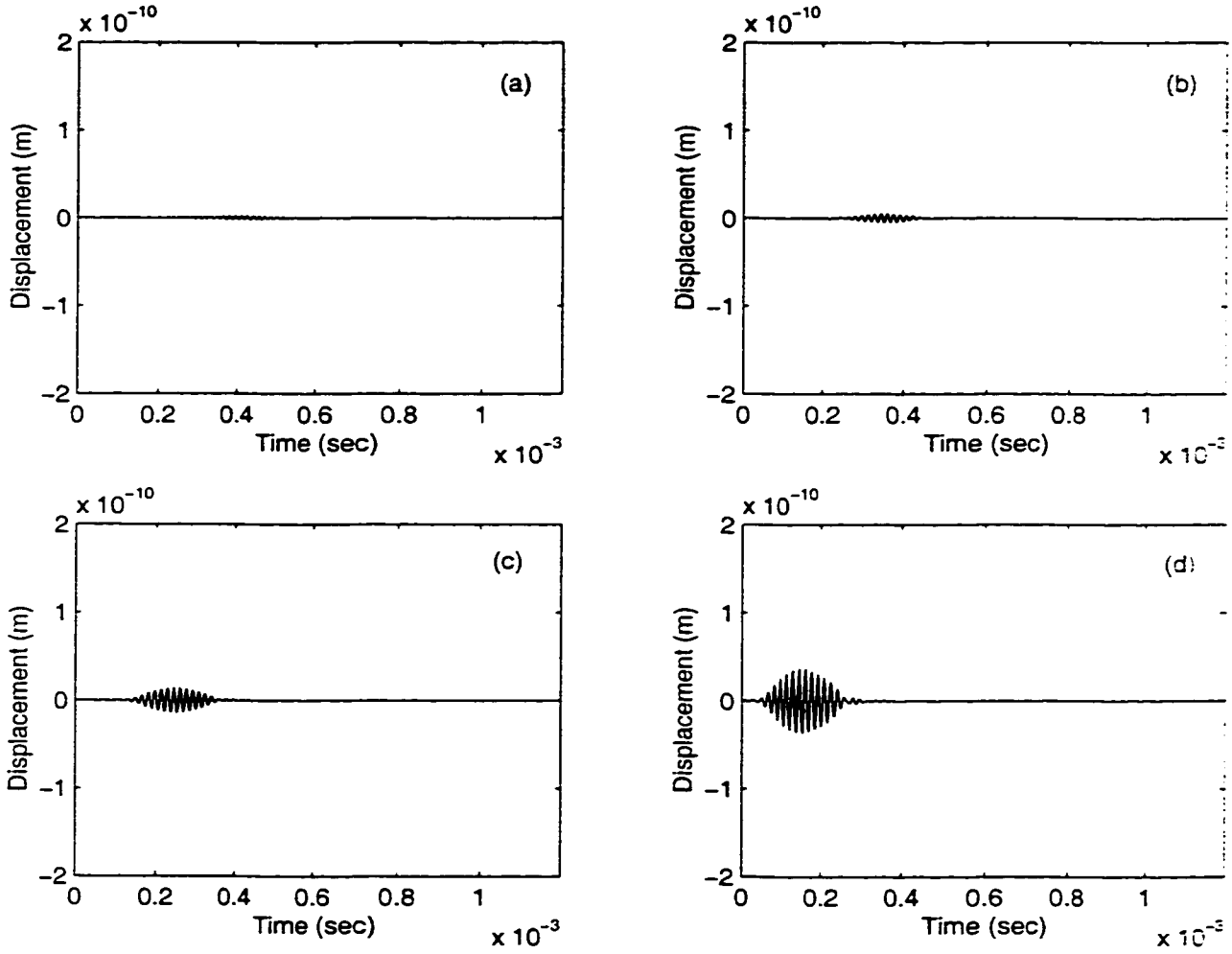

Figure 5.14: Response of constant thickness (0.03 m) cantilever Timoshenko beam at x= (a) $0.125m$ (b) $0.375m$ (c) $0.625m$ (d) $0.875m$ using throw-off element. using $\eta = 0.025$

are 8. For linearly varying thickness, the effect of throw-off element is more pronounced as shown in Figure (5.15). When both the width and thickness are varied linearly then the response of beam with throw-off element is much more damped as shown in Figure (5.16)) as compared to the cantilever beam (Figure (5.17)).

5.7 MODE INVESTIGATION

To investigate the modes of propagation, different values of η used here are 0.015, 0.01, 0.005, 0.001 and 0.0005. Clear from the Figures (5.18) to (5.22) of the beam response at various nodes, that there are two modes of wave propagation and reflection from the boundary. Second mode is faster than the first mode, so always ahead of it. At the force end, both modes overlap. As the wave propagates in the beam towards the fixed end, the two modes separate because of the difference in their velocities. It is clear that the distance between these two modes goes on increasing as they propagate until at a certain location where they are clearly distinguishable along with the visible reflection behind the first mode. But as they propagate further towards the fixed boundary, the effect of reflection starts acting on these modes. And at location very close to the fixed boundary the two modes, due to the strong reflection, they become inseparable from the reflection wave. Because of the overlapping with the

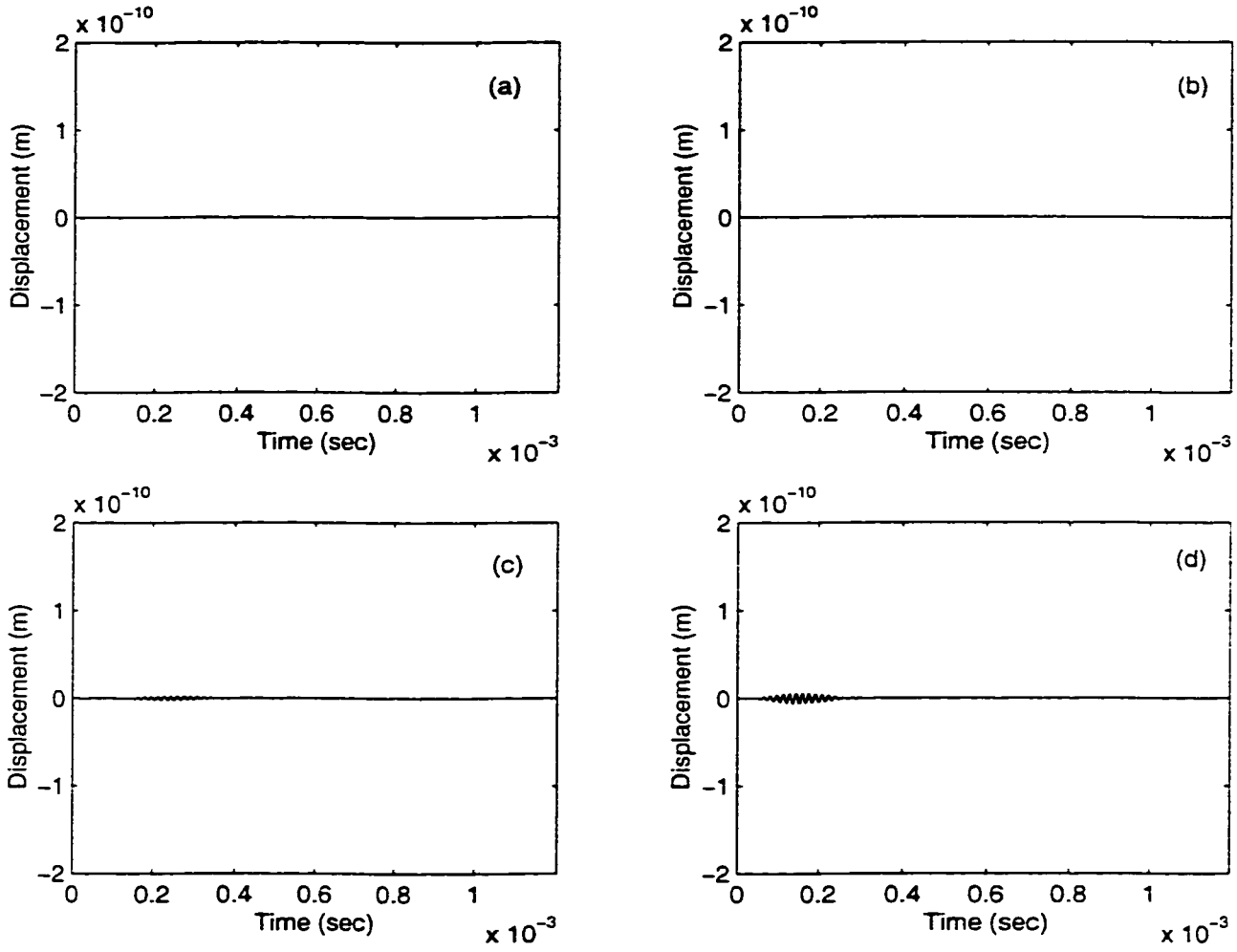

Figure 5.15: Response of linearly varying (for $TR = 0.14$) cantilever Timoshenko at x= (a) $0.125m$ (b) $0.375m$ (c) $0.625m$ (d) $0.875m$ beam using throw-off element. using $\eta = 0.025$

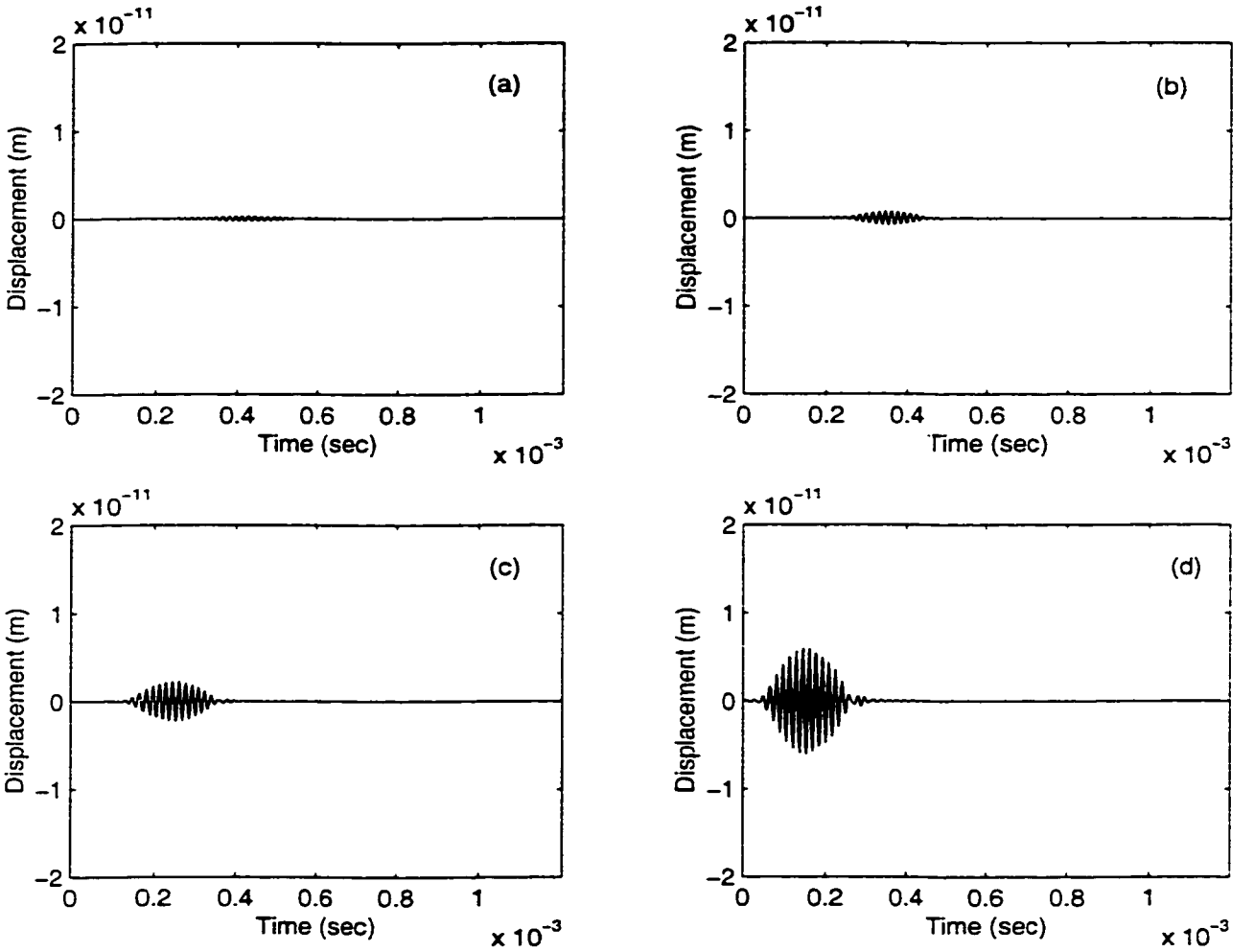

Figure 5.16: Response of cantilever Timoshenko beam with throw-off element, for $TR = 0.14$ *both in width and thickness*, at x= (a) $0.125m$ (b) $0.375m$ (c) $0.625m$ (d) $0.875m$, using $\eta = 0.025$

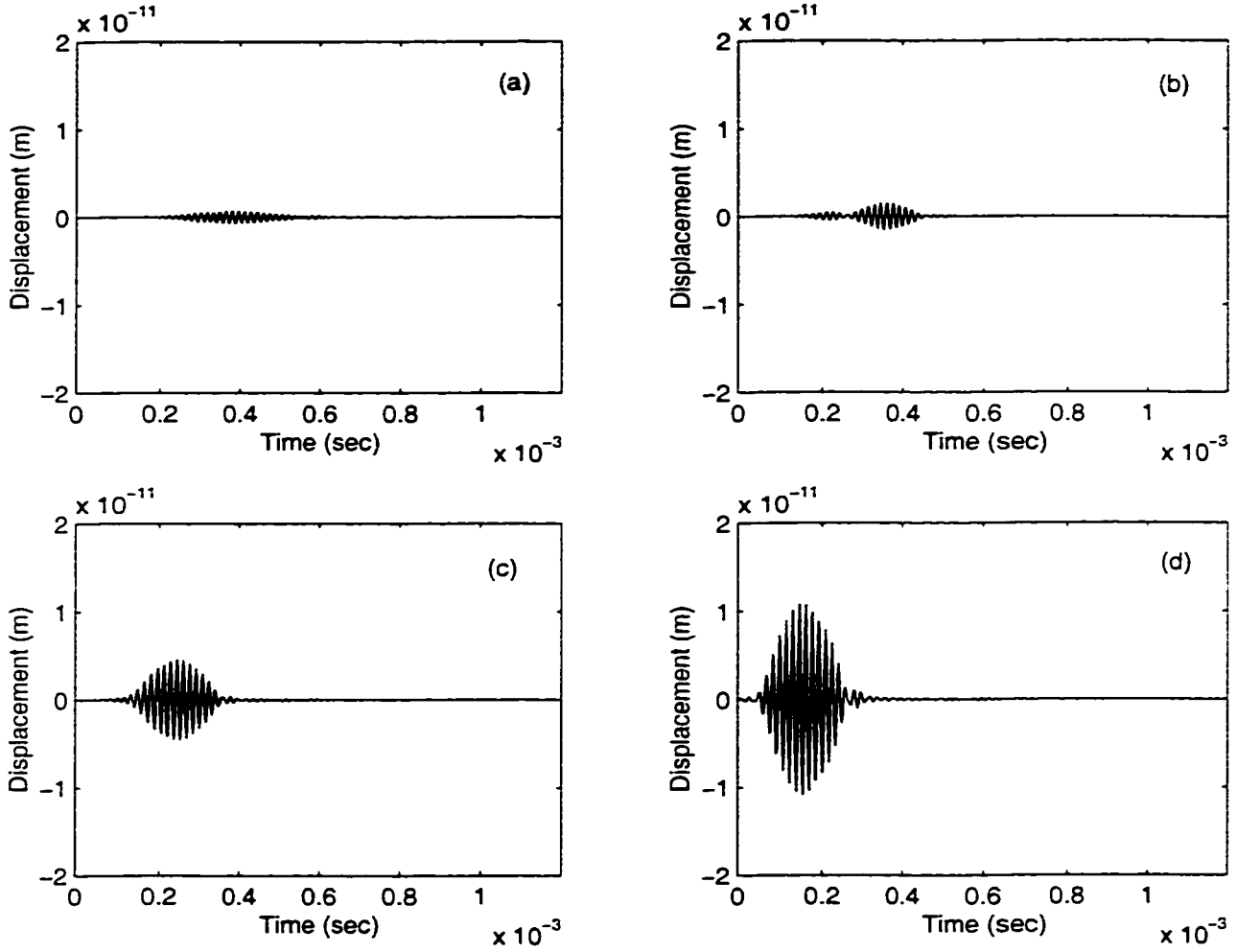

Figure 5.17: Response of cantilever Timoshenko beam, for $TR = 0.14$ *both in width and thickness*, at x= (a) $0.125m$ (b) $0.375m$ (c) $0.625m$ (d) $0.875m$, using $\eta = 0.025$

reflection pulse there, the amplitude of the pulse is increased than the alone first mode and reflection pulses. Throughout its passage, the second . mode doesn't show any effect of damping on its amplitude, unlike the first mode which shows decay in its amplitude during propagation. There is another pulse reflected from the force end of the cantilever beam and travelling in the direction of the forward moving pulse, as clear from the Figures (5.18) to (5.22). To investigate this reflection from the force end, the Figures (5.23) to (5.30) show the response of uniform thickness (0.05 m) Timoshenko beam of cantilever type boundary, with and without throw off element. At the force end this reflection is ahead of the reflection from the fixed end. Travelling through the beam reflection from the fixed end dies out behind the reflection from the fixed end. However, with throw off element only two major pulse are in picture; the incident forward pulse and the refection from the fixed end.

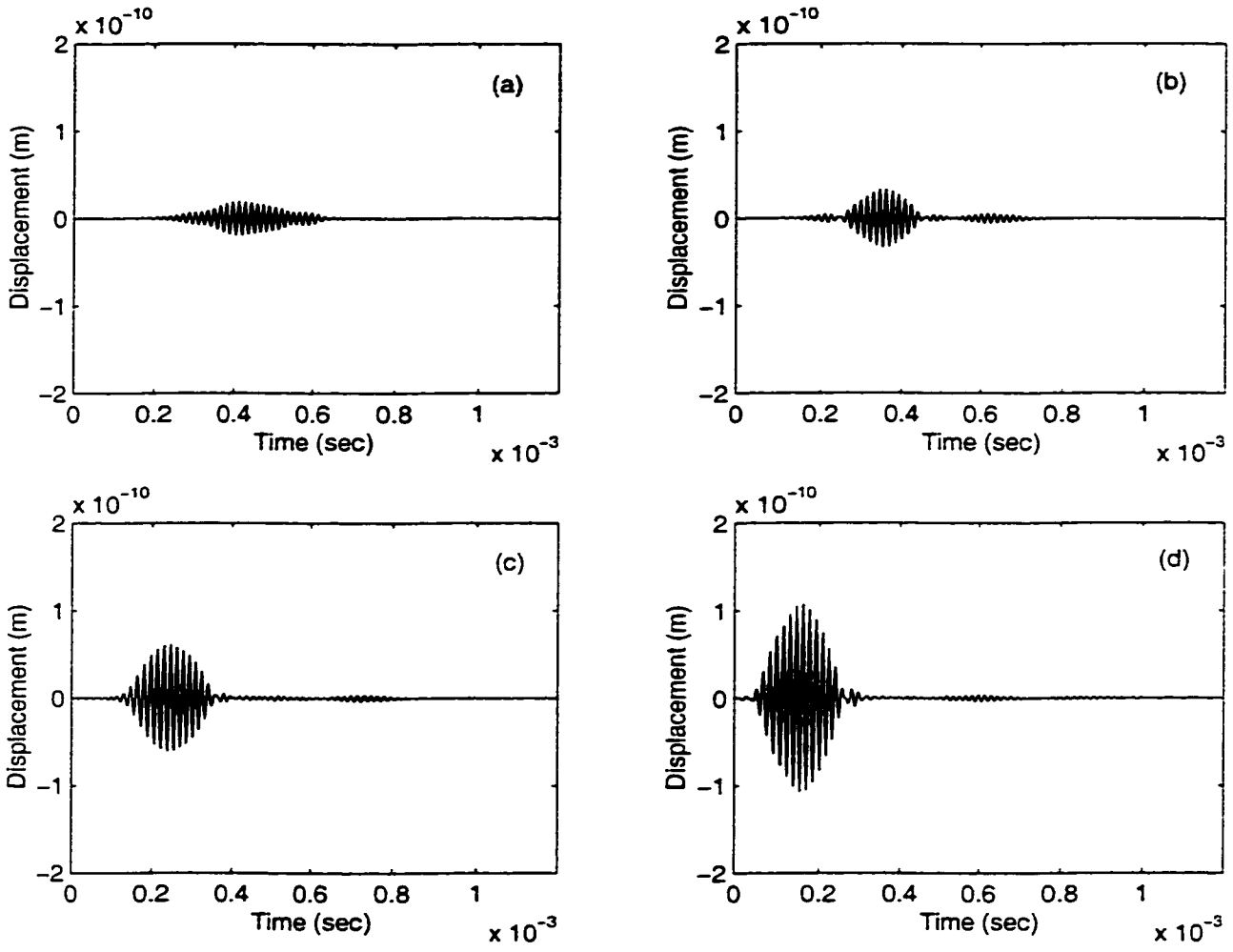

Figure 5.18: Response of cantilever Timoshenko beam, for $TR = 0.14$ at x= (a) $0.125m$ (b) $0.375m$ (c) $0.625m$ (d) $0.875m$, using $\eta = 0.015$

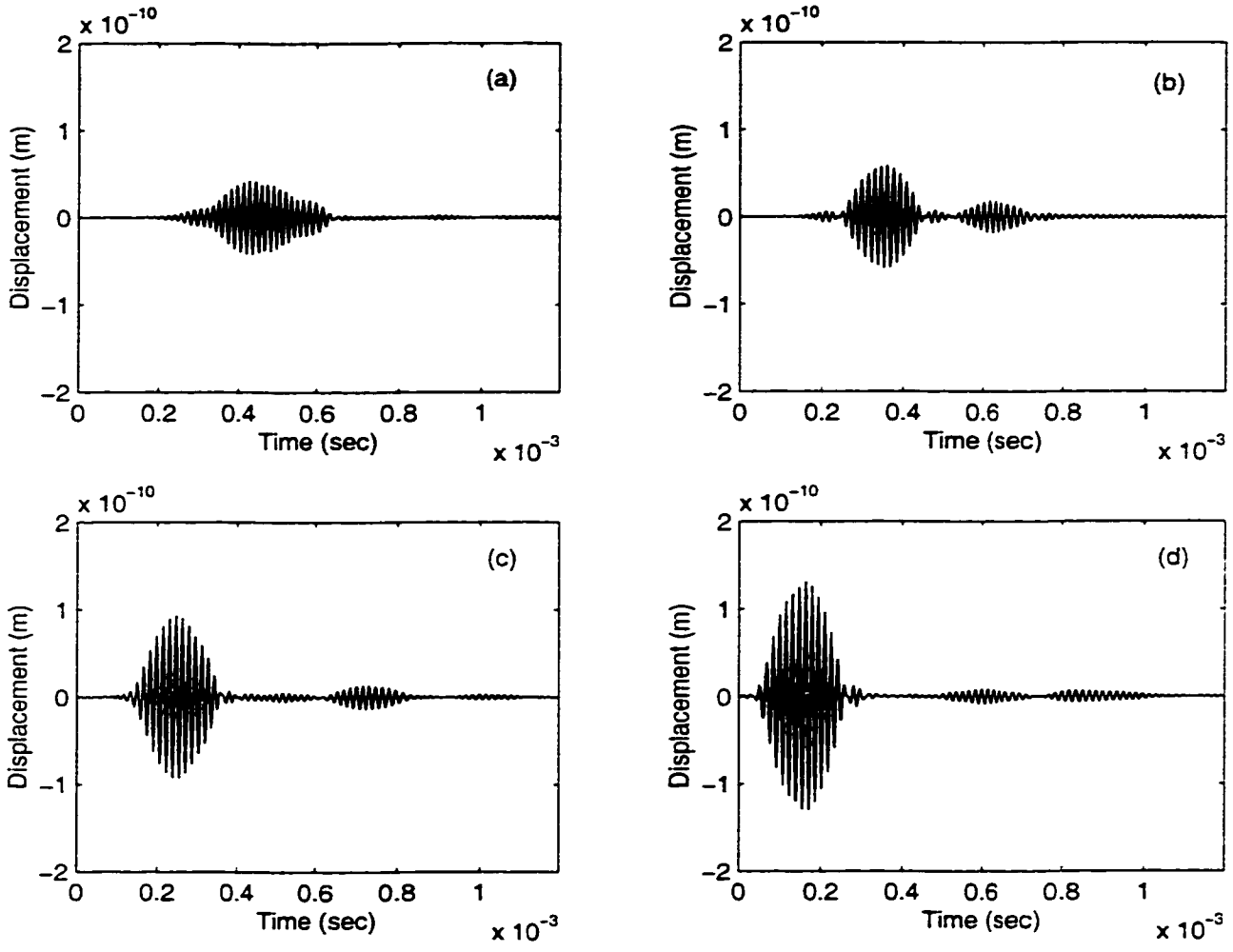

Figure 5.19: Response of cantilever Timoshenko beam, for $TR = 0.14$ at x= (a) $0.125m$ (b) $0.375m$ (c) $0.625m$ (d) $0.875m$, using $\eta = 0.01$

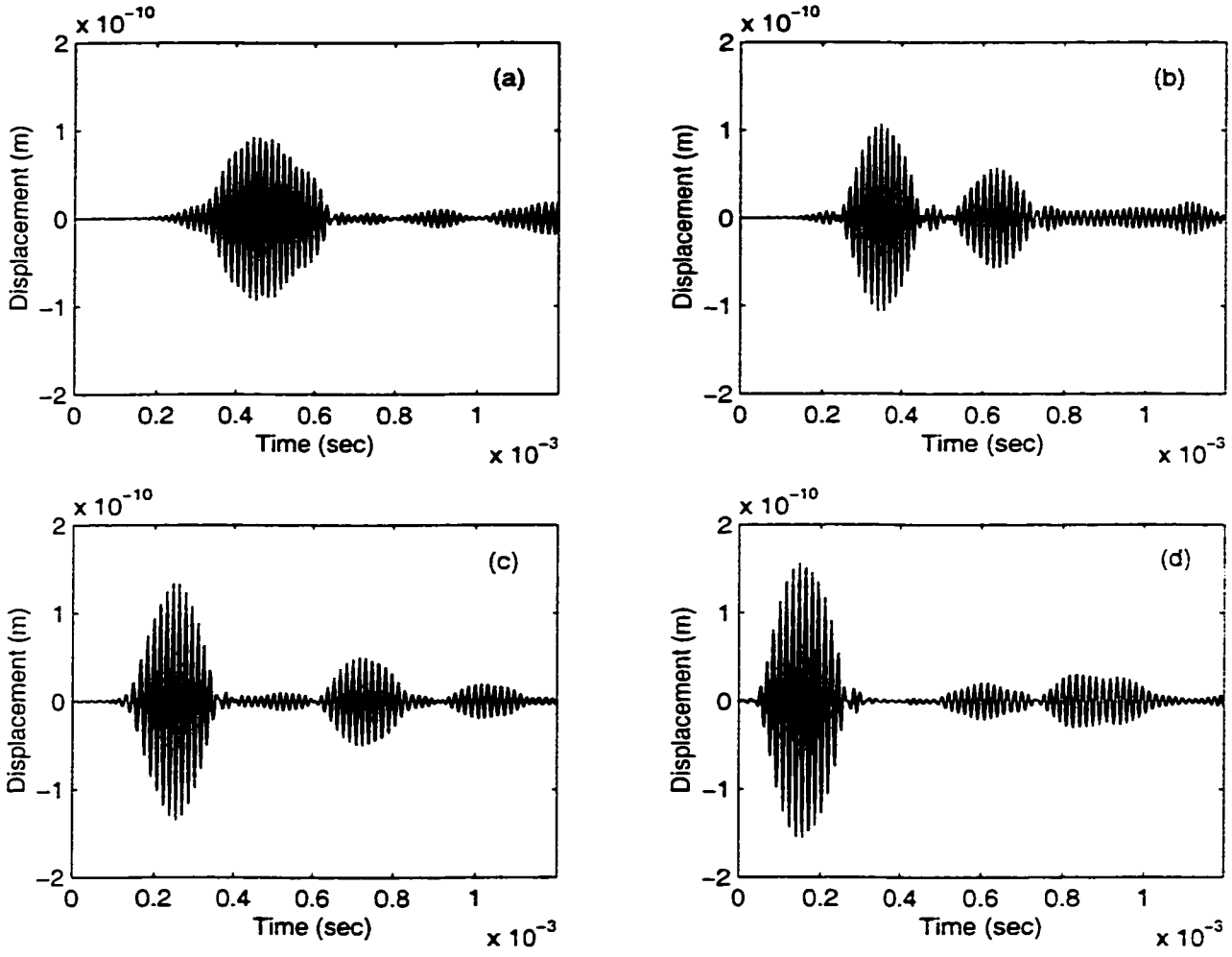

Figure 5.20: Response of cantilever Timoshenko beam, for $TR = 0.14$ at x= (a) $0.125m$ (b) $0.375m$ (c) $0.625m$ (d) $0.875m$, using $\eta = 0.005$

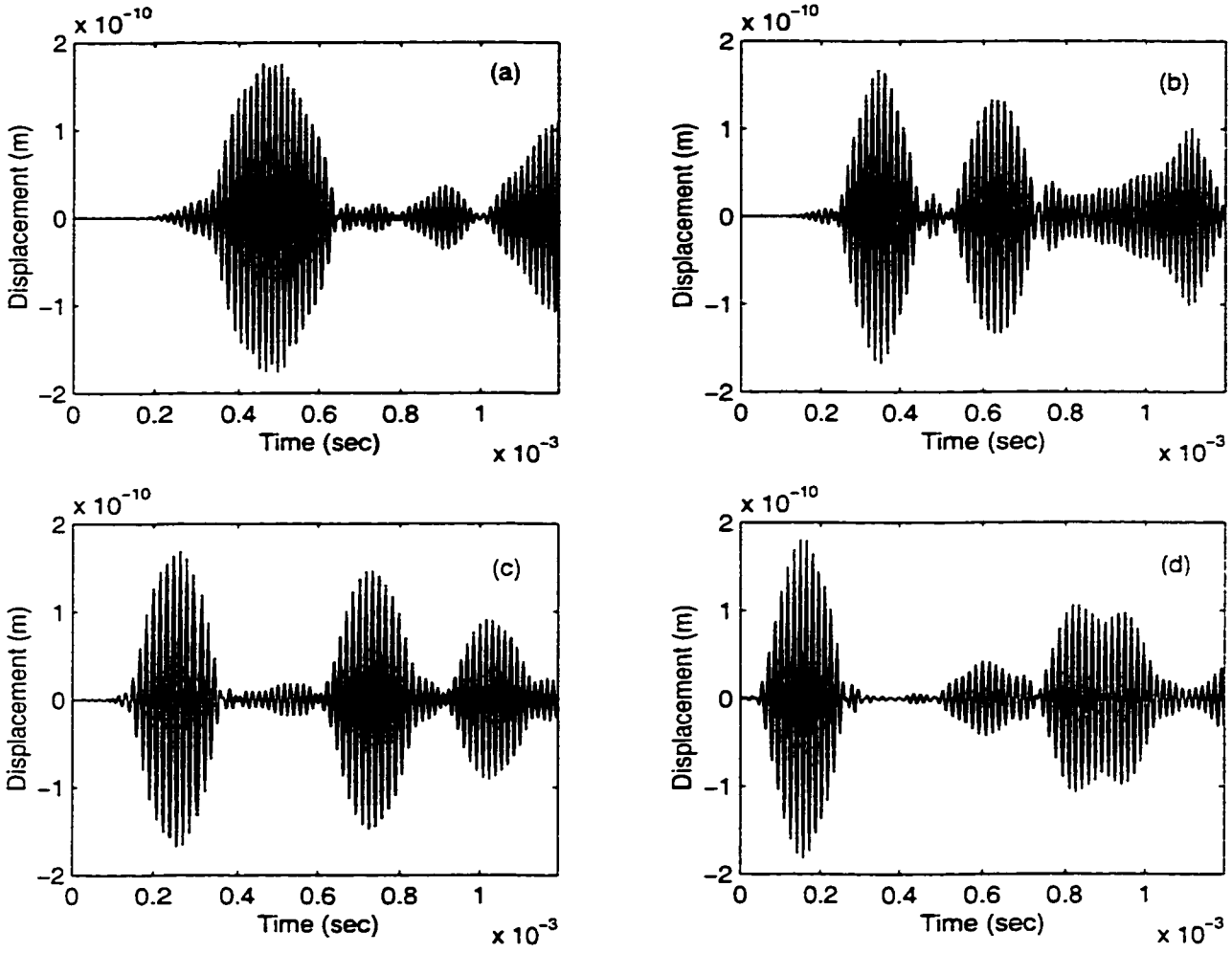

Figure 5.21: Response of cantilever Timoshenko beam, for $TR = 0.14$ at x= (a) $0.125m$ (b) $0.375m$ (c) $0.625m$ (d) $0.875m$, using $\eta = 0.001$

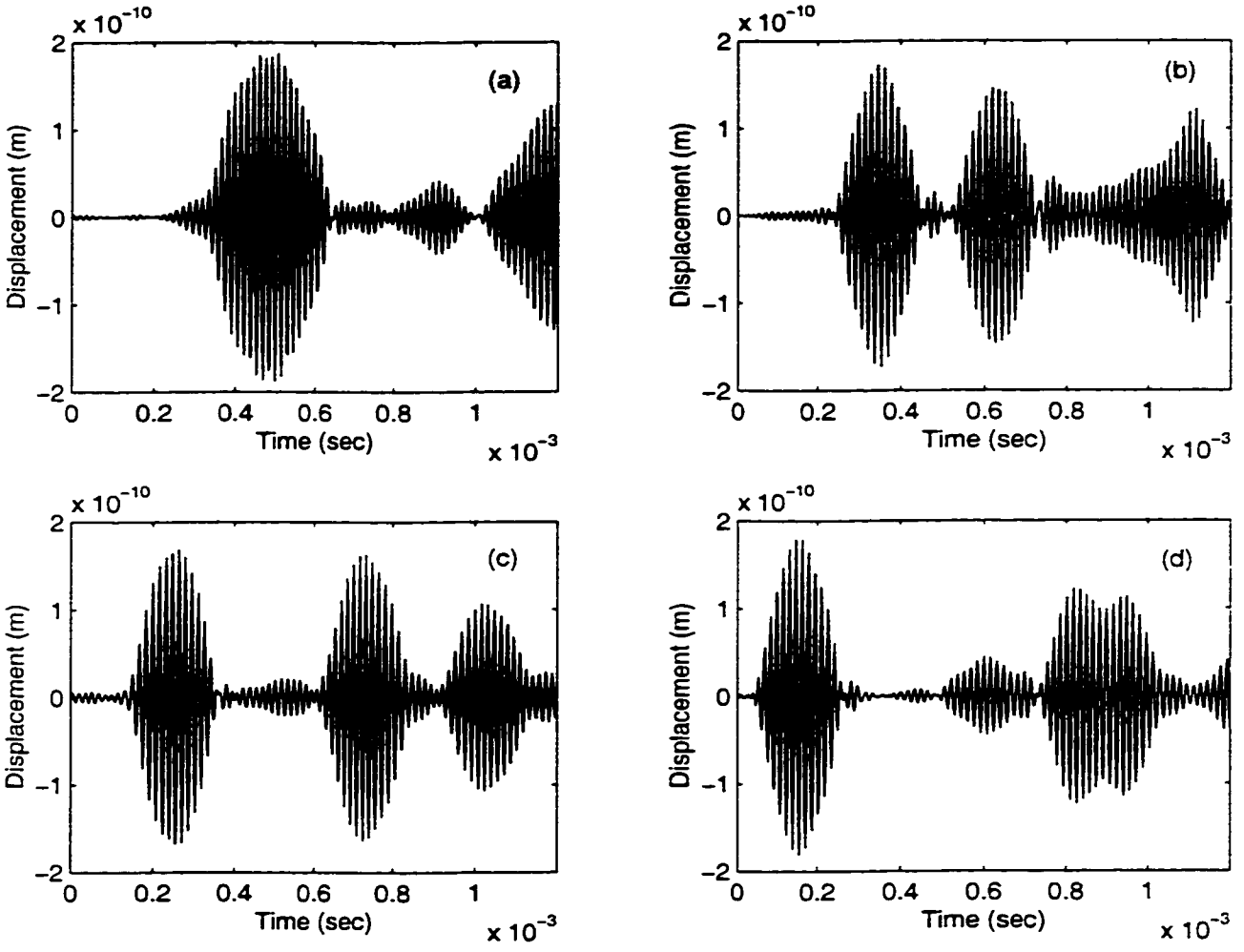

Figure 5.22: Response of cantilever Timoshenko beam, for $TR = 0.14$ at x= (a) $0.125m$ (b) $0.375m$ (c) $0.625m$ (d) $0.875m$, using $\eta = 0.0005$

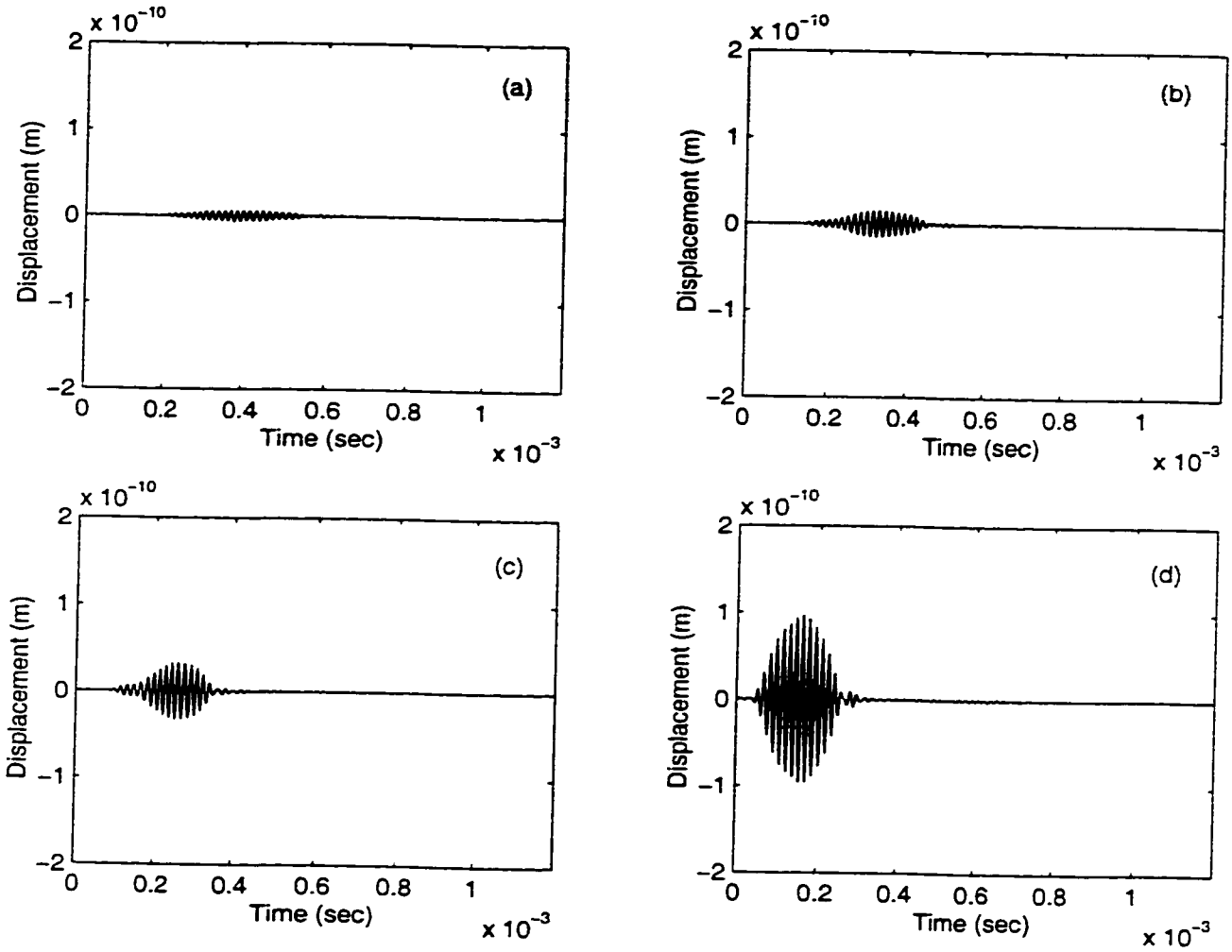

Figure 5.23: Response of uniform thickness ($0.05m$) cantilever Timoshenko beam at x= (a) $0.125m$ (b) $0.375m$ (c) $0.625m$ (d) $0.875m$, using $\eta = 0.025$

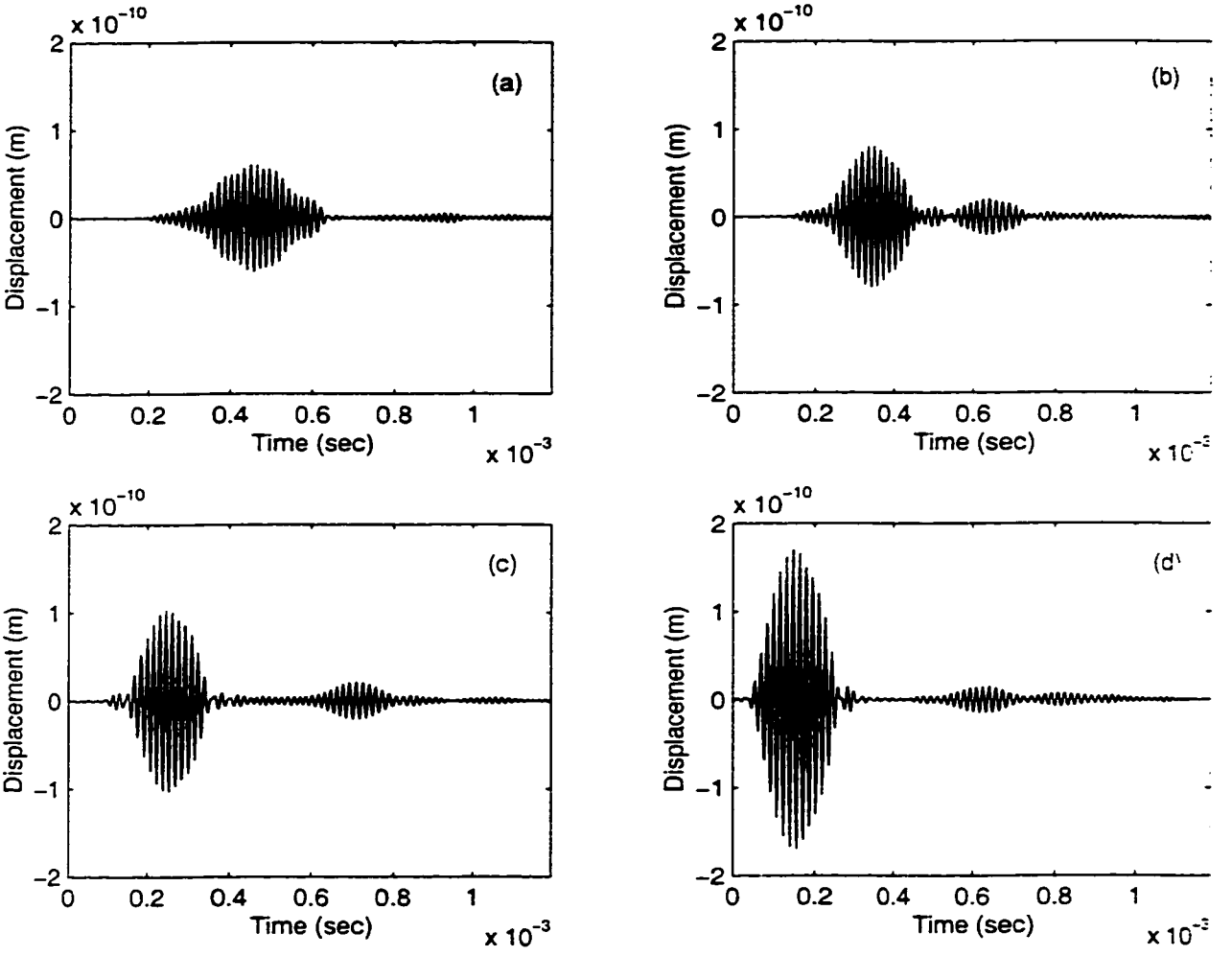

Figure 5.24: Response of uniform thickness ($0.05m$) cantilever Timoshenko beam at x= (a) $0.125m$ (b) $0.375m$ (c) $0.625m$ (d) $0.875m$, using $\eta = 0.01$

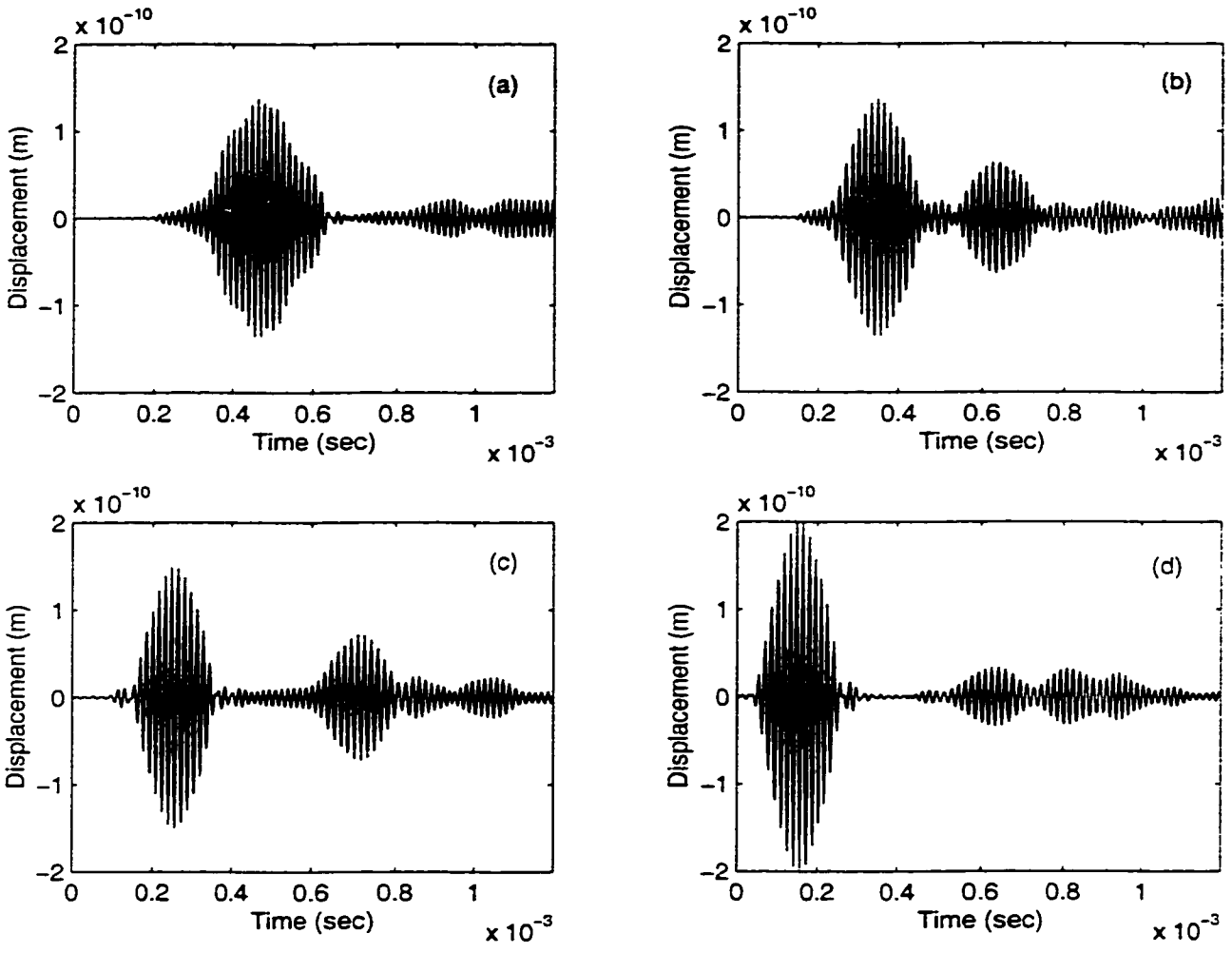

Figure 5.25: Response of uniform thickness ($0.05m$) cantilever Timoshenko beam at x= (a) $0.125m$ (b) $0.375m$ (c) $0.625m$ (d) $0.875m$, using $\eta = 0.005$

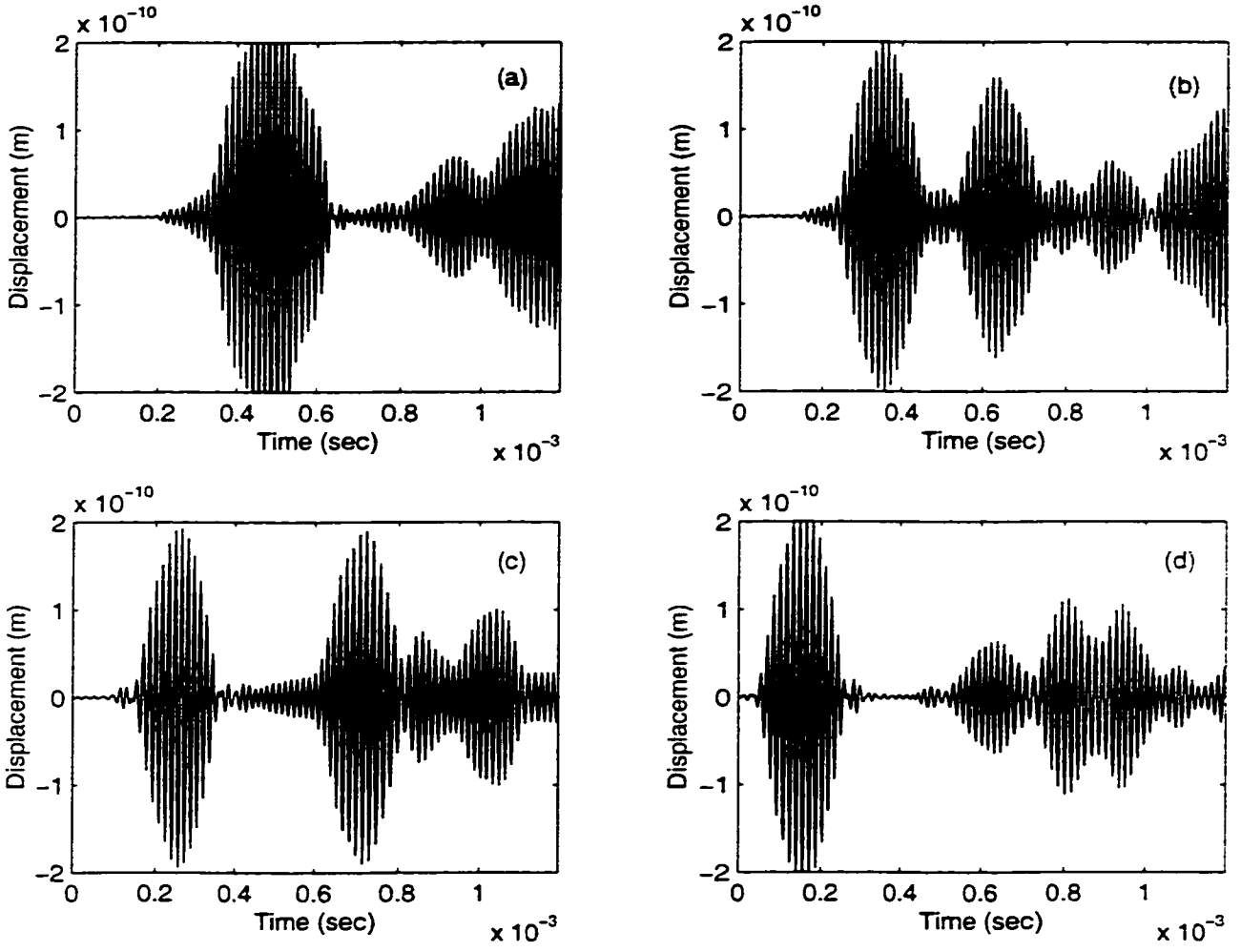

Figure 5.26: Response of uniform thickness ($0.05m$) cantilever Timoshenko beam at x= (a) $0.125m$ (b) $0.375m$ (c) $0.625m$ (d) $0.875m$, using $\eta = 0.001$

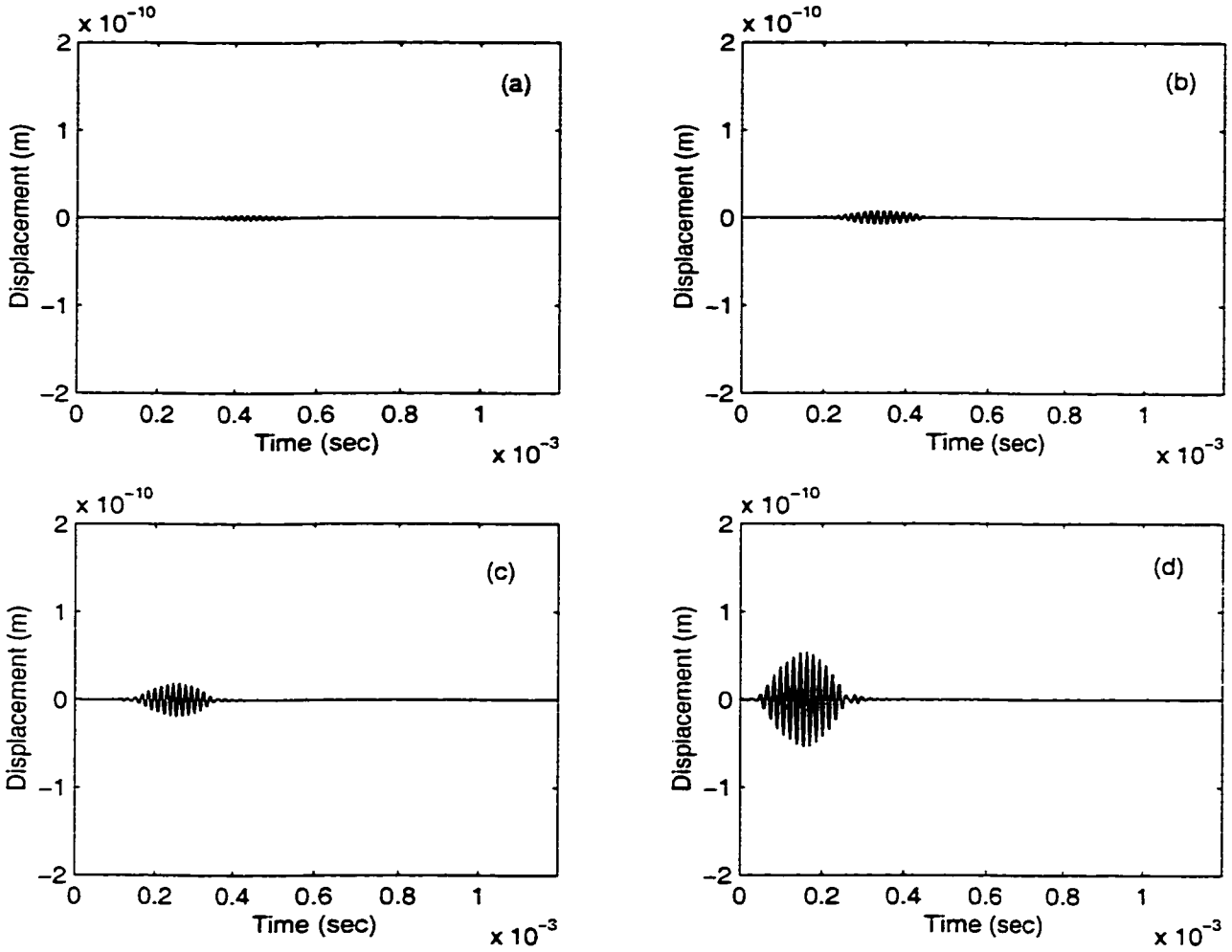

Figure 5.27: Response of uniform thickness ($0.05m$) cantilever Timoshenko beam with throw-off element at x= (a) $0.125m$ (b) $0.375m$ (c) $0.625m$ (d) $0.875m$. using $\eta = 0.025$

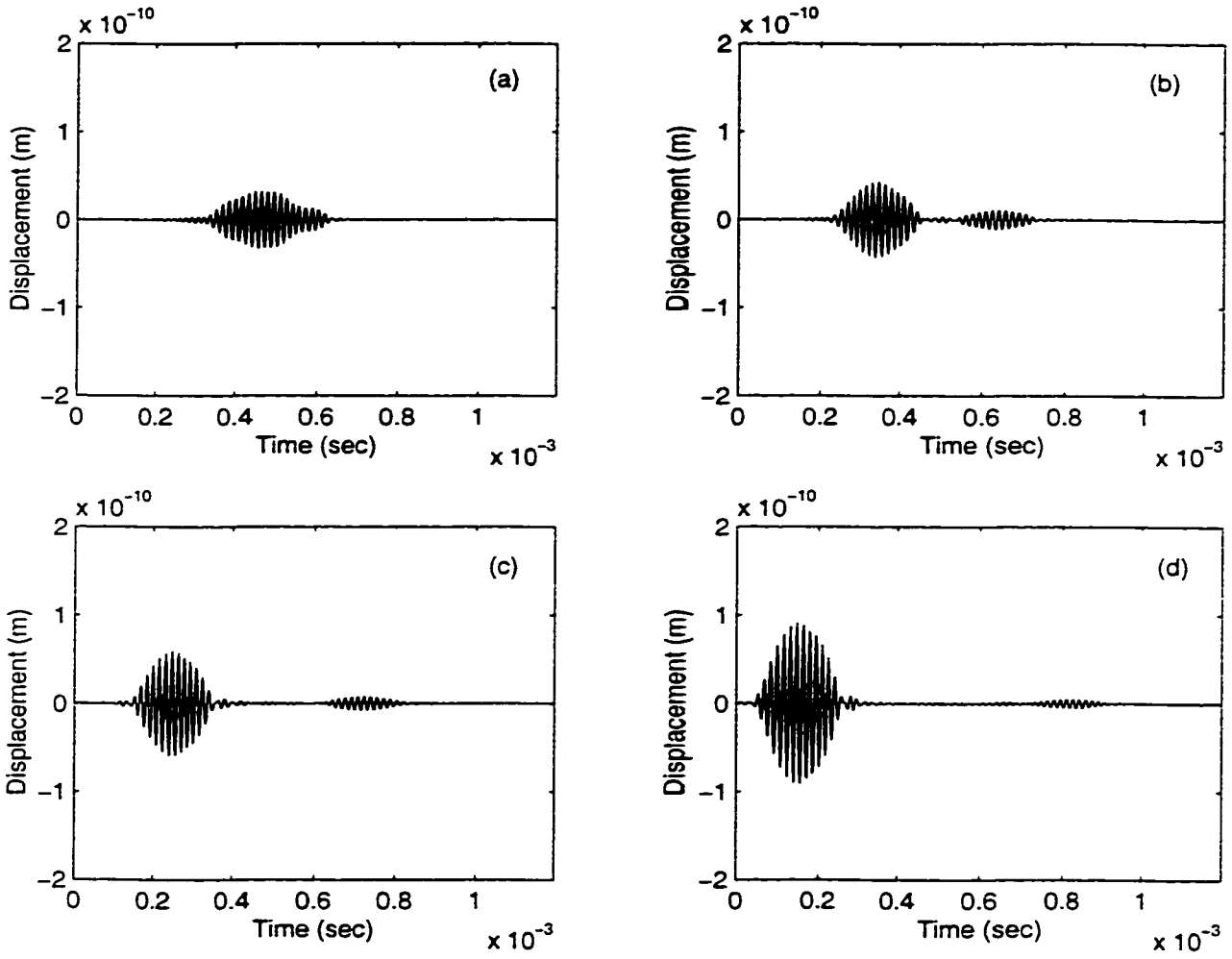

Figure 5.28: Response of uniform thickness ($0.05m$) cantilever Timoshenko beam with throw-off element at x= (a) $0.125m$ (b) $0.375m$ (c) $0.625m$ (d) $0.875m$, using $\eta = 0.01$

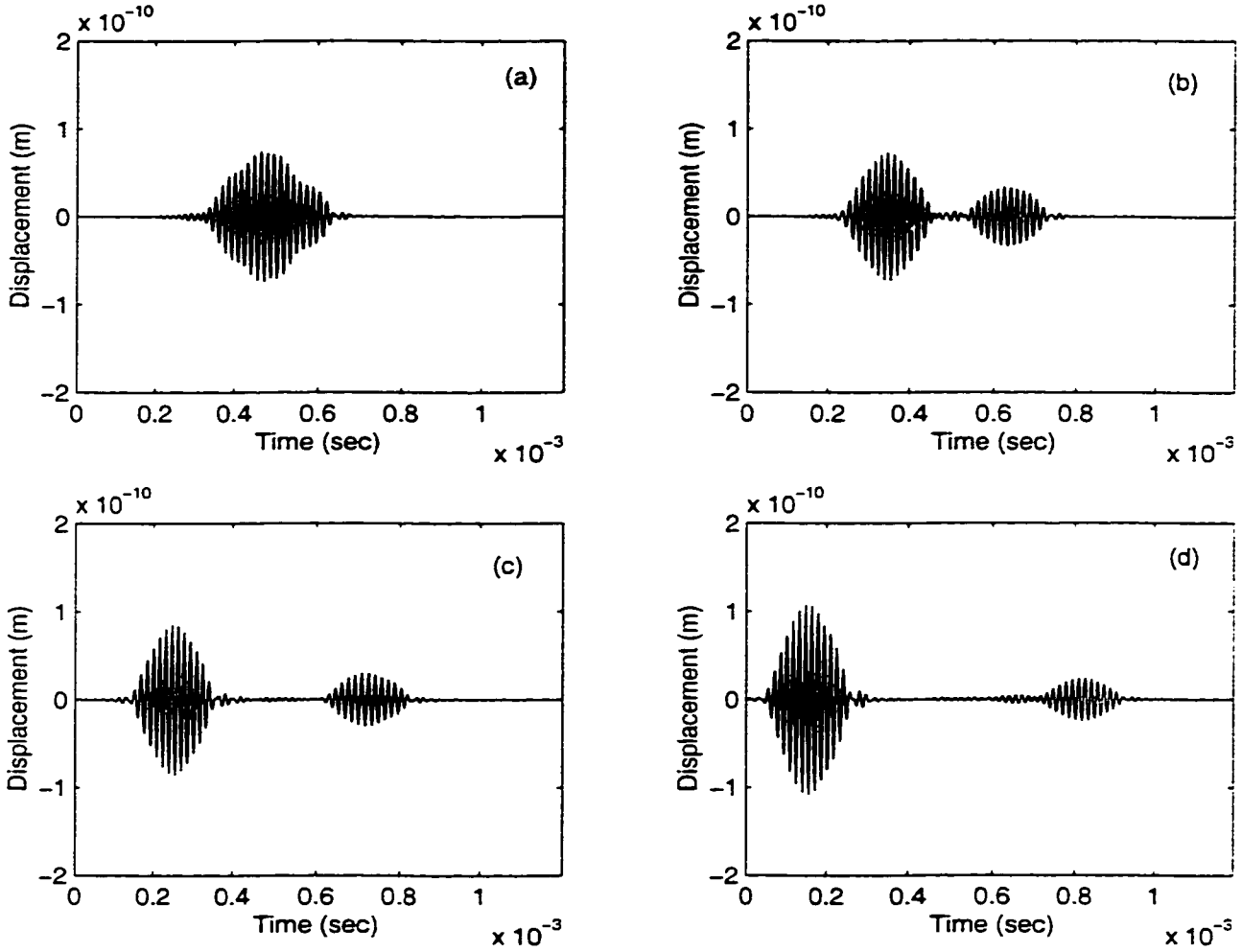

Figure 5.29: Response of uniform thickness ($0.05m$) cantilever Timoshenko beam with throw-off element at x= (a) $0.125m$ (b) $0.375m$ (c) $0.625m$ (d) $0.875m$. using $\eta = 0.005$

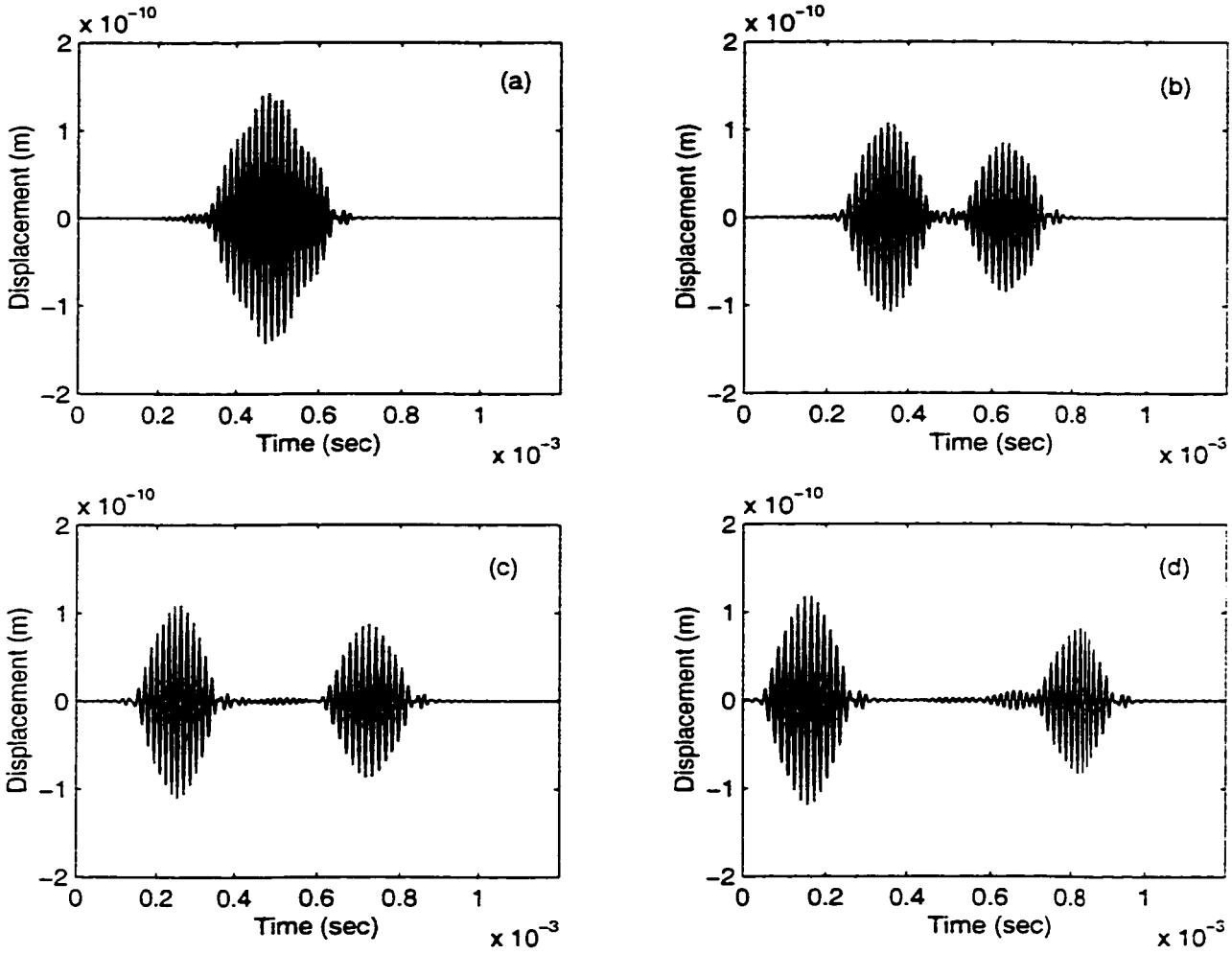

Figure 5.30: Response of uniform thickness ($0.05m$) cantilever Timoshenko beam with throw-off element at x= (a) $0.125m$ (b) $0.375m$ (c) $0.625m$ (d) $0.875m$, using $\eta = 0.001$

Chapter 6

CONCLUSION

Transient response of varying thickness Timoshenko beam under point load is studied here. Transient problem is converted to simple pseudo-static problem by transferring the equations of motion in frequency domain using FFT. After making use of Finite Element methodology, the frequency dependant response is obtained. The response is reconstructed in time domain by IFFT. The major conclusions drawn from the beam response studied above are:

- Spectral element formulation converts the dynamic problem into pseudo-static problem so the number of equations are not reduced
- Since the spectral element formulation treats the mass distribution exactly so no need of extra mass matrix, thus saving in memory space

- Because of exact mass distribution wave propagation within each element is treated exactly
- For uniform thickness there is no need of subdividing the beam into elements
- Existence of a critical taper ratio is observed in clamped free beam where the pattern of displacement is changed
- The number of elements needed for convergence is proportional to the propagation distance.
- Infinite or very long beams can be handled easily by using throw-off elements.
- The power spectrum of the excitation signal must be low-banded for stability purposes.
- It is noticed that the second mode has weak normal displacement component.
- There is no considerable effect of damping on the amplitude of the second mode.
- The amplitude of first mode is larger than that of second mode.due to the fact that first mode represents the flexural motion.
- Reflection wave also composed of two modes of differing speed just like the forward wave.

- The group velocity of the first mode in cantilever beam doesn't show any regular pattern of change with change in taper ratio, TR.
- The Group velocity of the first mode in simply supported timoshenko beam shows approximately constant values at various TR.
- The group velocity of the first mode in simply supported beam is higher than that for the cantilever beam.

A wide field is open for the future research in the above work. Some of such future potentials are:

- Possible use of polynomial forms of thickness variation
- Use of isoparametric elements
- Derivation of dispersion relation for varying thickness Timoshenko beams
- Use of more D.O.F.
- Experimental determination of optimal damping value

Bibliography

[1] R. P. Goel. Transverse vibrations of tapered beams. *Journal of sound and vibration*, 47(1):1–7, 1976.

[2] P. K. Roy and N. Ganesan. Studies on the dynamic behaviour of a cantilever beam with varying thickness. *Journal of Sound and Vibration*. 177(1):1-13. 1993.

[3] M. ASCE Bing Y. Ting. Beam on elastic foundation finite element. *Journal of Structural Engineering*. 110:2324-39. Oct 1984.

[4] W. Carnegie et al. An improved method of matrix displacement analysis in vibration problems. *The Aeronautical Quarterly*. pages 321-332. November 1969.

[5] Yew Chin Lai et al. Dynamic response of beams on elastic foundation. *Journal of structural engineering*, 118(3):853–858, March 1992.

[6] S. P. Timoshenko. On the correction for shear of the differential equation for transverse vibrations of prismatic bars. *Philosophical Magazine*.

41(6):744–746, 1921.

[7] M. A. Dangler and M. Goland. Transverse impact of long beams, including rotary inertia and shear effects. In *Proceedings of the First U.S. National Congress of Applied Mechanics*, pages 179–186, New York. 1951. The American Society of Mechanical Engineers.

[8] Kanwar K. Kapur. Vibration of a timoshenko beam, using finite element approach. *The Journal of the Acoustical Society of America*, 40(5):1058–1063, 1966.

[9] D. M. Egle. An approximate theory for transverse shear deformation and rotary inertia effects in vibrating beams. Technical report. General Electric company, 1969.

[10] Franklin Y. Cheng and Chris P. Pantelides. Dynamic timoshenko beam columns on elastic media. *Journal of structural engineering*, 114(7):1524–50, July 1988.

[11] C. W. S. To. A linearly tapered beam finite element incorporating shear deformation and rotary inertia for vibration analysis. *Journal of Sound and Vibration*, 78(4):475–484, 1981.

[12] T. Nakao et al. Theoretical and experimental analysis of flexural vibration of the viscoelastic timoshenko beam. *Journal of Applied Mechanics*, 52:728–732, 1985.

[13] G. R. Heppler and J. S. Hansen. Timoshenko beam finite elements using trignometric basis functions. *AIAA Journal*, 26(1):1378–1386, 1988.

[14] J. Thomas and B. A. H. Abbas. Finite element model for dynamic analysis of timoshenko beam. *Journal of Sound and Vibration*, 41(3):291–299, 1975.

[15] Y. C. Hou and C. H. Tseng. A new high order non-uniform timoshenko beam finite element on variable two parameter foundations for vibration analysis. *Journal of Sound and Vibration*, 191(1):91–106, 1996.

[16] G. M. Lindberg. Vibration of non-uniform beams. *The Aeronautical Quarterly*, November 1963.

[17] Calif et al. Flexural wave solutions of coupled equations representing the more exact theory of bending. *Journal of Applied Mechanics*, pages 511–514, 1953.

[18] Usik Lee and Joonkeun Lee. Dynamic continuum modeling of truss type space structures using spectral elements. *Journal of Spacecraft and Rockets*, 33(3):404–409, 1996.

[19] James F. Doyle. A spectrally formulated finite element for longitudinal wave propagation. *Int. Journal of Analytical and Experimental Modal Analysis*, 3:1–5, 1987.

[20] James F. Doyle. *Wave propagation in Structures*. Springer-Verlag, 1989.